FINAL TECHNICAL

to

Air Force Office of Scientific Research

for project entitled

Advanced Ceramics from Liquid Solution

Grant No.: AFOSR-F49620-94-1-0071
Inclusive Dates: 1 December 1993 to 30 November 1997

PRINCIPAL INVESTIGATOR

John D. Mackenzie, Professor
Department of Materials Science and Engineering
Phone: (310) 825-3539
FAX: (310) 206-7353

January, 1998

REPORT DOCUMENTATION PAGE

OMB No. 0704-0188

1. AGENCY USE ONLY (Leave blank)	2. REPORT DATE	3. REPORT TYPE AND DATES COVERED
	January 1998	Final Technical Report

4. TITLE AND SUBTITLE

Advanced Ceramics from Liquid Solutions

5. FUNDING NUMBERS

F49620-94-1-0071
2303/BS
61102F

6. AUTHOR(S)

J.D. Mackenzie

7. PERFORMING ORGANIZATION NAME(S) AND ADDRESS(ES)

Air Force Office of Scientific Research/NL
110 Duncan Avenue, Suite B-115
Bolling Air Force Base
Washington, D.C. 20332-0001

8. PERFORMING ORGANIZATION REPORT NUMBER

9. SPONSORING/MONITORING AGENCY NAME(S) AND ADDRESS(ES)

Univ of California, Los Angeles
Dept of Materials Science & Engineering
6531 Boelter Hall
Los Angeles, CA 90095-1595

10. SPONSORING/MONITORING AGENCY REPORT NUMBER

11. SUPPLEMENTARY NOTES

12a. DISTRIBUTION/AVAILABILITY STATEMENT

Approved for public release;
distribution unlimited.

12b. DISTRIBUTION CODE

13. ABSTRACT *(Maximum 200 words)*

This Final Technical Report for the period from 1 December 1993 to 30 November 1997 presents a summary of research performed on two classes of materials prepared by the sol-gel method. The first class of materials is the Ormosils. Work has been carried out on the structure and mechanical properties of Ormosils and a model was presented to account for the dependence of properties on structures, especially for the rubbery Ormosils. The high-temperature stability of rubbery Ormosils was found to be enhanced by the presence of small amounts of iron ions. A method was developed for the introduction of carbon black into Ormosils. Aerogels of 95% porosity were known to be extremely fragile. By the incorporation of polydimethyl siloxane, the resultant Ormosils were rendered rubbery. The second family of materials investigated consisted of ferroelectric thin films. Single crystals of $KNbO_3$ films were grown by the sol-gel method, etched to form waveguides and shown to emit green light when impinged upon by infrared lasers due to second harmonic effects. A theory was postulated which enabled the understanding of ferroelectric behavior shown by amorphous oxide films. A technique was developed for the successful growth of multilayed stack of alternating oxide films. A new family of organic-inorganic hybrids which showed ferroelectric behavior was discovered by the involrporation of an organic dye, TDP, into the SiO_2 network of a gel containing minute crystallites of $LiNbO_3$ or $BaTiO_3$.

14. SUBJECT TERMS	15. NUMBER OF PAGES
Sol-Gel Science, Organic-Inorganic Hybrids, Ferroelectrics, Ormosils	46
	16. PRICE CODE

17. SECURITY CLASSIFICATION OF REPORT	18. SECURITY CLASSIFICATION OF THIS PAGE	19. SECURITY CLASSIFICATION OF ABSTRACT	20. LIMITATION OF ABSTRACT
Unclassified			

TABLE OF CONTENTS

ABSTRACT

This Final Technical Report for the period from 1 December 1993 to 30 November 1997 presents a summary of research performed on two classes of materials prepared by the sol-gel method. The first class of materials is the Ormosils. Work has been carried out on the structure and mechanical properties of Ormosils and a model was presented to account for the dependence of properties on structures, especially for the rubbery Ormosils. The high-temperature stability of rubbery Ormosils was found to be enhanced by the presence of small amounts of iron ions. A method was developed for the introduction of carbon black into Ormosils. Aerogels of 95% porosity were known to be extremely fragile. By the incorporation of polydimethyl siloxane, the resultant Ormosils were rendered rubbery. The second family of materials investigated consisted of ferroelectric thin films. Single crystals of $KNbO_3$ films were grown by the sol-gel method, etched to form waveguides and shown to emit green light when impinged upon by infrared lasers due to second harmonic effects. A theory was postulated which enabled the understanding of ferroelectric behavior shown by amorphous oxide films. A technique was developed for the successful growth of multilayed stack of alternating oxide films. A new family of organic-inorganic hybrids which showed ferroelectric behavior was discovered by the involrporation of an organic dye, TDP, into the SiO_2 network of a gel containing minute crystallites of $LiNbO_3$ or $BaTiO_3$.

1. Introduction

This grant was awarded in December 1, 1993. The main objective was to prepare two families of advanced ceramic materials based on the liquid solution approach. The first family of advanced ceramics to be synthesized was ferroelectric thin films such as $BaTiO_3$ and $LiNbO_3$. The technique selected was the sol-gel method. Under this general heading of "ferroelectrics" it was proposed that three separate but related tasks would be performed. These were (a) the preparation of single crystals, (b) the preparation of amorphous ferroelectrics and (c) the preparation of multilayered structures based on alternating conductive and insulating films. The second family of advanced ceramics to be investigated was supposed to be that based on silicon nitride. However, early in 1994, because of the potential usefulness of Ormosils (organically modified silicates) as thermal insulation for rocket motors and the interests of the Phillips Laboratory at the Edwards Air Force Base, permission was obtained from Captain Hugh de Long to postpone research on silicon nitride and to perform research on the Ormosils instead. This progress report covers the entire period of the grant from 1 December 1993 to 30 November 1998.

2. Research on Ormosils

Most of our research on Ormosils are based on the reactions between tetraethoxy silane (TEOS) and polydimethylsiloxane (PDMS). Different ratios of TEOS to PDMS are reacted according to the method shown in Figure 1. In the past four years, our research on Ormosils can be conveniently divided five parts.

(a) Structure and Mechanical Properties

When PDMS is added to TEOS, the mechanical properties of the resultant Ormosils change continuously as shown by Figure 2. Some actual values of mechanical properties are shown in Table 1 for the rubbery Ormosils. At low PDMS concentrations, the Ormosils are hard, brittle solids.

Table 2 shows the values of H/K_c where H is the Vickers hardness and K_c is the fracture toughness. This ratio is defined as the index of brittleness. When the PDMS reaches 10 wt.%, the brittleness of the silica gel has decreased by 50%. These 'hard" Ormosils are some 5 to 8 times harder than most organic plastics. Figure 3 gives the Vickers Hardness as a function of PDMS content. A theory was developed to enable the calculation of hardness. The agreement between experimental and calculated values of hardness is excellent as shown in Figure 3. The structural changes to the silica network as a result of the chemical reaction between TEOS and PDMS are depicted by Figures 4 and 5. The hard Ormosil structure is presented in Figure 4(b) and the rubbery Ormosil structure is given in Figure 5. The rubbery behavior is explained by the mechanism of coiling and uncoiling of the PDMS chains linking the clusters of SiO_2 as illustrated in Figure 6. At present, various industrial laboratories are evaluating the potentials of hard Ormosils as abrasion resistant coatings for organic plastics.

(b) High-Temperature stability of Rubbery Ormosils

Since a rubbery Ormosil may contain as much as 70 wt.% of SiO_2, it is natural to inquire as to the possibility of preparing new high temperature stable rubbers with Ormosils. As prepared, the PDMS-SiO_2 rubbery Ormosils would maintain their rubbery property even after a few hours of heating at 200°C in air. Although this is better than common rubber, it is necessary to inquire why the rubbery behavior of Ormosils should be lost at temperatures in excess of 200°C and if there are methods to make improvements of the high temperature stability. During the period of this grant, we discovered that very small amounts of iron added to the original Ormosil liquid solution in the form of $FeC\ell_3$, or Fe_2O_3, can increase the thermal stability of Ormosil very significantly. Figure 7 shows the remarkable effects of small amounts of Fe. The presence of Fe appears to be ineffective in N_2. It may therefore be presumed that the oxidation of the CH_3 groups on the PDMS chains causes the loss of rubbery elasticity. Iron is also known to endow high temperature

Table 1 - Mechanical Properties of Rubbery Ormosils at 20°C

Samples	Density (g/cm^3)	Tensile Strength (MPa)	Elongation (%)	Elastic Modulus (MPa)	Resilence (%)
$TEOS/PDMS_{1700}$	0.46	2.15	24.5	19.2	47
Aerosil ox50-$TEOS/PDMS_{1700}$**	0.79	0.86	42.6	3.0	69
Aerosil 90*-$TEOS/PDMS_{1700}$	0.83	1.58	38.3	7.0	72
Aerosil 150-$TEOS/PDMS_{1700}$	0.87	1.58	33.2	7.8	73
Aerosil 200- $TEOS/PDMS_{1700}$	0.91	1.63	23.2	11.7	72
Aerosil ox50-$TEOS/PDMS_{4200}$	0.79	1.15	51.3	4.0	69
Aerosil 90- $TEOS/PDMS_{4200}$	0.80	1.82	49.6	10.0	70
Aerosil 150-$TEOS/PDMS_{4200}$	0.81	2.25	34.7	11.5	72
Aerosil 200-$TEOS/PDMS_{4200}$	0.84	2.41	34.7	13.5	72

* The number for each Aerosil type indicates the BET surface area ± 15 in units of m^2/g.
The average primary particle sizes of Aerosils in nm are 40, 20, 14 and 12 for Aerosil ox50, 90, 150 and 200, respectively.

** The subscripts **1700** and **4200** are the molecular weights of $PDMS_{1700}$ and $PDMS_{4200}$, respectively.

Table 2 Indices of Brittleness of the Hard Ormosils

Wt.% of PDMS	0	3	5	8	10
Mol.% of $[Si(CH_3)_2O]$	0	7.9	12.8	19.5	23.7
Fracture toughness (Mpa $m^{1/2}$)	0.501 ± 0.002	0.492 ± 0.002	0.479 ± 0.001	0.465 ± 0.001	0.460 ± 0.001
Brittleness ($\mu m^{-1/2}$)	3.63 ± 0.15	3.19 ± 0.13	2.86 ± 0.11	2.32 ± 0.12	1.88 ± 0.12

stability in organic polymers. It has been suggested that some of the iron ions exist in the Fe^{2+} state. These Fe^{2+} ions will use up oxygen molecules and convert to Fe^{3+} state and thus less oxygen will be available to react with the CH_3 groups. This type of explanation is unsatisfactory since the ratio of the amount of Fe ions to CH_3 groups can be only 0.001 and the Fe is already effective (see Figure 7). At present, an acceptable mechanism for the effective influence of Fe ions is not known. We have found that another transition metal ion, vanadium, is also effective in enhancing high temperature stability although it is not as pronounced as Fe.

(c) Ormosils as High Temperature Insulators - Collaboration with Edwards Air Force Base

During this grant period, we have collaborated with Dr. J. Lichtenhan of the Phillips Laboratory at the Edwards Air Force Base to fabricate and to test Ormosils as insulators for rocket motors. Large sheets of Ormosils were fabricated and submitted to the Phillips Laboratory for testing. Such samples are shown in Figure 8. The testing method is illustrated in Figure 9. The initial results were promising. However, the tensile strengths of the Ormosil samples were relatively low and created a problem for handling when the insulation is applied to the rocket motor casing. Because of the lack of human resources we were unable to continue with experiments to strengthen the Ormosils which remain to be a promising family of insulation materials for high temperature applications.

(d) Additions of Carbon Black to Ormosils

Because the additions of carbon black to organic rubber can cause large changes of mechanical properties, it was logical to consider the effects on Ormosils. Three types of carbon black were obtained from the Degussa Corporation: SB4, SB5 and FW200 have average particle sizes of 25, 20 and 13 nm, respectively. It was impossible to add more than 3 wt.% of carbon black

to the Ormosil solution because of agglomeration. The method developed is shown in Figure 10. The compositions studied and the density and porosity results of the filled Ormosils are shown in Table 3. Samples containing the FE200 were blue in color, presumably because of Rayleigh Scattering from the ultrafine carbon particles (13 nm). The samples containing the larger carbon particles were gray in color resulting from a combination of scattering and absorption. The mechanical properties of Ormosils were found to be significantly influenced by the concentration and the size of the carbon black particles. Table 4 shows the FW200 can affect the tensile strength, elongation and elastic modulus of Ormosils more than the larger particle carbons. Table 5 shows the influence of carbon concentration. In Figure 11, tensile strength is plotted against carbon black concentration and in Figure 12, resilience is shown as a function of carbon black type and concentration.

Although both the tensile strengths and resilience of Ormosils can be increased significantly via the addition of 2 wt.% of carbon black, the increases are relatively minor as compared to the influence of carbon black on common organic rubbers. Secondly, the process shown by Figure 10 is highly complex and it will not be cost-effective for large scale preparation. Much more research will have to be done if serious applications of Ormosils are contemplated in the future.

(e) Rubbery Aerogels

Aerogels made from the supercritical drying of SiO_2 gels can have more than 99% porosity and are known as the best thermal insulator ever synthesized. Because of the brittleness of SiO_2 and the low mechanical strengths of such a porous solid, aerogels have not been used widely as a thermal insulator. Since the brittleness of silica gel can be greatly reduced by network structural modification via the incorporation of polydimethylsiloxane PDMS chains, this research was undertaken to study the preparation and properties of rubbery "aero-Ormosils" or "Aeromosil." Two methods were developed to synthesize these new materials and shown

Table 3 Density and Porosity of Carbon Black filled ORMOSILs

Material	Measured Density ρ_b (gm/cm^3)	Calculated Fully Dense Material Density ρ_1 (g/cm^3)	Calculated Porosity ρ_1 (g/cm^3)
60/40 ORMOSIL	0.45	1.29	0.65
ORMOSIL with 1 wt.% SB4	0.49	1.30	0.62
ORMOSIL with 2 wt.% SB4	0.56	1.31	0.57
ORMOSIL with 3 wt.% SB4	0.58	1.32	0.56
ORMOSIL with 2 wt.% SB5	0.89	1.31	0.48
ORMOSIL with 1 wt.% FW200	0.75	1.30	0.42
ORMOSIL with 2wt.% FW200	1.01	1.31	0.23
ORMOSIL with 3 wt.% FW200	1.03	1.32	0.22

Table 4 Mechanical Properties of FW200, SB5, and SB4 ORMOSILs

Material	Strength (Mpa)	Elongation (%)	Elastic Modulus (MPa)
ORMOSIL with 2 wt.% FW200 (primary particle size: 13nm)	2.50	4.50	27.4
ORMOSIL with 2 wt.% SB5 (primary particle size: 20 nm)	1.05	5.8	10.3
ORMOSIL with 2 wt.% SB4 (primary particle size: 25 nm)	0.89	16.1	8.1

Table 5 Mechanical Properties of ORMOSILs with Increasing Loading

Material	Strength (MPa)	Elongation (%)	Elastic Modulus (MPa)
ORMOSIL with 1 wt.% SB4	0.64	8.1	5.8
ORMOSIL with 2 wt.% SB4	0.89	15.1	8.1
ORMOSIL with 3 wt.% SB4	0.90	16.1	8.1
ORMOSIL with 1 wt.% FW200	1.40	11.2	23.6
ORMOSIL with 2 wt.% FW200	2.50	4.5	27.4
ORMOSIL with 3 wt.% FW200	2.58	4.5	29.9

in Figure 13. The supercritical drying equipment is shown in Figure 14. The bulk density, porosity and specific surface area of some aeromosils are shown in Table 6. Pore size distributions for the acid and the acid/base catalyzed samples are shown in Figure 15. That the Aeromosils are indeed rubbery is shown in the three photographs of Figure 16. The sample is shown to have been reduced in length by 25% and then recovered fully. A tentative model to explain this rubbery behavior is presented in Figure 17. Rubbery Aerogels are thus a reality. For practical applications, a method will have to be developed for the cost-effective production of rubbery aerogel pellets rather than sheets.

3. Research on Ferroelectrics

Our research on ferroelectrics via the sol-gel method has been concentrated on both crystalline and amorphous thin films. The program is basically a continuation of our previous effort under AFOSR-91-0096 which terminated on 30 November 1993. The most important aspect of our program is the discovery of ferroelectricity in new organic-inorganic hybrid materials. Our program is summarized in the four separate sections below.

(a) Single Crystal Ferroelectrics

Single crystalline films of $KNbO_3$ were successfully grown epitaxially on MgO and $SrTiO_3$ substrates. Figure 18 shows the lattice fringe image of $KNbO_3$ on $SrTiO_3$. Narrow channels were etched into the films to form waveguides as shown in Figure 19. Infrared laser beams of 1.06 μm were directed into the film and green light of 0.532 μm was generated via second harmonic modes. Fe was also introduced into the sol-gel solutions as dopants for the $KNbO_3$. The third-order susceptibility of the doped film now enabled the intensity amplification of laser light as shown in Figure 20. We have therefore demonstrated conclusively that the sol-gel method can be used to fabricate ferroelectric single crystal films with useful second-order and third-order nonlinear optical properties.

Table 6 Bulk density with corresponding porosity and specific surface area with linear correlation coefficient from BET

Sample	Density (g/cm^3)	Porosity (% theory)	SSA (m^3/g)	Correlation
OA2	0.071	96.8	1169	0.9969
10A3	0.061	97.2	1370	0.9993
10A2	0.059	96.6	1274	0.9990
10A3	0.057	96.7	1193	0.9990
20A2	0.066	95.6	818	0.9997
20A3	0.051	96.6	786	0.9993
0AB2	0.079	96.4	1103	0.9991
10AB2	0.099	94.3	920	0.9995
20AB2	0.150	90.1	659	0.9996

(b) Multilayered Thin Film Structures

It has been proven for covalent semiconductors that a multilayered structure consisting of alternating layers of insulator and semiconductor can result in a "quantum well." Such quantum wells hold promise for many devices in photonics. The equivalent multilayered structures with oxides had not been fabricated. During this grant period, an automatic dip-coating equipment was designed and constructed (Figure 21). Two solutions A and B are placed in separate containers standing on a rotating platform. The substrate first dips into A and is then hoisted slowly upwards into a furnace. After the film A is heat-treated, the substrate is then lowered into solution B and the process repeated. The speed of the dipping can be controlled. We were able to prepare multilayers of amorphous $BaTiO_3$ and SiO_3 to test the utility of the equipment. Up to 12 pairs of films with thickness of the order or 300Å each were fabricated as shown in Figure 22. The optical quality of the stack was excellent. Due to the shortage of human resources, we were unable to continue with this program.

(c) Amorphous Ferroelectric Films

In our previous AFOSR Grant No. AFOSR-91-0096 we first reported that amorphous $LiNbO_3$ film prepared by the sol-gel method exhibited ferroelectric behavior. During this period such "amorphous ferroelectricity" was confirmed for $BaTiO_3$ and PZT. The presence of "ferrons"--extremely small crystals of the order of 20Å--was confirmed by high resolution electron microscopy and proposed to be responsible for the observed ferroelectric behavior. A model was generated to account for this anomalous behavior. The model involves the coupling of dipoles via ferrons and the non-crystalline part of the solid network as illustrated in Figure 23. A comparison of experimental ferroelectric properties and those calculated based on this model was very satisfactory as presented in Table 7. Table 8 gives a comparison of the properties of polycrystalline film, amorphous film and

Table 7- Theoretical results in comparison with experimental results

	PZT		$BaTiO_3$	
	Theoretical	*Experimental*	*Theoretical*	*Experimental*
Free energy $G-G_o$ (J/mol)	-38	no	-3.7	no
Averaged value of dipole moments of ferrons, $<\mu_Z>$, (10^{-28} C cm)	17.2	22.55 (crystal)	7.8	17.7 (crystal)
Remanent polarization P_r ($\mu C/cm^2$) from statistical thermodynamics	3.2	3.2	2.3	2.3
Remanent polarization P_r ($\mu C/cm^2$) from statistical physics	3.9	3.2	2.1	2.3
Coercive field E_c (10^4V/cm)	5.0	7.8	6.5	10.5
Permittivity of ferrons ε_r	no	1850 (crystal)	no	210 (crystal)
Permittivity of porous matrix ε_r	98	160 (overall)	75	90 (overall)
Permittivity of dense matrix ε_r	165	no	140	no
Volume fraction of ferron ν_1 (%)	16.3	10 or more (HRTEM)	17.6	10 or more (HRTEM)
Porosity of overall film ν_p (%)	9.2	no	10.3	no
Refractive index of ferrons η_F	no	2.70 (crystal)	no	2.40 (crystal)
Refractive index of dense matrix η_s	2.32	no	2.23	no
Refractive index of porous matrix η_m	2.1	2.1	2.0	2.0

Table 8 Electrical Properties of Polycrystalline and Amorphous $BaTiO_3$ Thin Films at Room Temperature (Some data of Ceramic bulk are listed for comparison)

Properties	Polycrystalline (850°C/6h)	Amorphous (400°C/1h)	Ceramic Bulk (1450°C/1h)*
Film's thickness t	0.3 mm	0.3 mm	
Average grain size (Å)	1000	no grains were	> 4000
Dielectric permittivity ε (25°C)	210 (1 kHz)	90 (1 kHz)	1400 (1kHz)
Resistivity (d.c.) ρ (Ωcm)	5.5×10^9	1.5×10^9	**
Pyroelectric coefficient ρ (nC/cm^2K)	10	0.5	20
Remanent polarization P_r(C/cm^2)	19	2.3	26
Coercive field E_c (kV/mm)	10	10	
Breakdown strength E_b (kV/mm)	800	> 60	**
Optical refractive index n	2.3	2.0	2.43 (n_o)*** 2.37 (n_e)***

* Data come from Ref. [1]
** Depends on dopants and processing
*** Data from single crystal

bulk ceramic $BaTiO_3$. The amorphous ferroelectric film appears to be a "weak" or "soft" ferroelectric.

(d) Organic-Inorganic Hybrids

During this grant period, we prepared thin amorphous films from solutions containing the double alkoxides of $LiNbO_3$ (and/or $BaTiO_3$) as well as TEOS. Our gelation and drying, the films manifested ferroelectric behavior and "ferrons" were again observed. This prompted us to examine gels made from solutions containing the $LiNbO_3$ (and/or $BaTiO_3$) double alkoxide, TEOS and TDP, a complex dye the structure of which is shown in Figure 24. On gelation, the TDP and TEOS would yield a silica network and ferrons of the $LiNbO_3$ (and/or $BaTiO_3$) would be trapped in the network. Electrical interactions would perhaps be possible between the ferrons as depicted in Figure 25. Ferroelectric behavior was indeed observed as shown by the P-E hysteresis loop in Figure 26. Ferrons were also revealed by high resolution electron microscopy as shown in Figure 27. We also discovered that the interactions between TDP and $LiNbO_3$ and $BaTiO_3$ are different as shown by the color difference of the films in Figure 28. The reasons for the different behavior of $LiNbO_3$ and $BaTiO_3$ are not known and investigations are on-going. These organic-inorganic hybrids constitute a new family of electronic materials and are worthy of further studies.

4. Cumulative Publications based on this Grant

Bescher, E.P., Mackenzie, J.D., Ohtsuki, T., Peyghambarian, N., "Rare Earth Organic Dye Nanocomposites by the Sol-Gel Method," MRS Symp. **351**, 135-139 (1994).

Cheng, Chih-Hsing, Xu, Yuhuan, Mackenzie, J.D., "The Growth of Epitaxial and Polycrystalline $KNbO_3$ Films via Sol-Gel Process," Ferroelectrics, **152**, 31-36 (1994).

Xu, Yuhuan, Chen, Chih-Hsing, Mackenzie, J.D., "Electrical Characterizations of Polycrystalline and Amorphous Thin Films of $Pb(Zr_xTi_{1-x})O_3$ and $BaTiO_3$ Prepared by Sol-Gel Technique," J. Non-Crystalline Solids, **176**, 1-17 (1994).

Mackenzie, J.D., "Organically Modified Ceramics by the Sol-Gel Method," Advanced Materials '93, Vol. **VI**, 753-761, ed. by S. Somiya, M. Doyama, R. Roy, Elsevier (1994).

Mackenzie, J.D., "Sol-Gel Optics III," SPIE Vol. **2288** (1994).

Yuh, S.K., Bescher, E., Mackenzie, J.D., "Luminescence of Trivalent Erbium in Low-Hydroxyl Gels," SPIE Proc. Vol. **2288**, 248-254 (1994).

Cheng, C.H., Xu, Y., Mackenzie, J.D., "Epitaxial Growth of $KNbO_3$ and Fe-Doped $KNbO_3$ Films via Sol-Gel Processing," SPIE Proc. Vol. **2288**, 445-455 (1994).

Xu, Y., Cheng, C.H., Mackenzie, J.D., "Optical and Electrical Properties of Polycrystalline and Amorphous PZT Thin Films by the Sol-Gel Method," SPIE Proc. Vol. **2288**, 456-467 (1994).

Wu, C., Xu, Y., Mackenzie, J.D., "Amorphous Multilayer Thin Films by Auto-Dip-Coating Technique," SPIE Proc. Vol. **2288**, 504-515 (1994).

Kramer, S.J., Mackenzie, J.D., "Thermal Stability Enhancement of Rubbery ORMOSILs," in: **Better Ceramics Through Chemistry VI**, Materials Research Society Proc., Vol. **346**, ed. by A.K. Chectham, C.J. Brinker, M.L. Mecartney and C. Sanchez, MRS, Pittsburgh, 709-714 (1994).

Mackenzie, J.D., Kao, Y.H., "Sol-Gel Process for Glass Integrated Optics," SPIE Critical Reviews **53**, 83-113 (1994).

Mackenzie, J.D., Kao, Y.H., "Transparent Glass Nanocomposites and Their Nonlinear optical Properties," Otto Schott Colloquium, ed. C. Russell, Glastech. Ber. **67C**, 50-54 (1994).

Thorne, K.J., Johnson, S.E., Zheng, H., Hawthorne, M.F., Mackenzie, J.D., "A Chemically Designed, UV Curable Polycarbosilane Polymer for the Production of Silicon Carbide Fibers and Monoliths," Chemistry of Materials, **6**[2], 110-115 (1994).

Mackenzie, J.D., "Nonlinear Optical Materials by the Sol-Gel Method," J. Sol-Gel Sci and Tech. **1**, 70-79 (1993).

Mackenzie, J.D., "Structures and Properties of Ormosils," J. Sol-Gel Sci and Tech. **2**, 81-86 (1994).

Morita, K., Hu, Y., Mackenzie, J.D., "Effects of Ultrasonic Irradiation on Preparation and Properties of Ormosils," J. Sol-Gel Sci. and Tech. **3**, 109-116 (1994).

Kao, Y.H., Hu, Y., Zheng, H., Mackenzie, J.D., "Second Haromic Generation in Transparent $BaTiO_3$ Glass-Ceramics," J. Non-Crystalline Solids **167**, 247-254 (1994).

Iwamoto, T., Mackenzie, J.D., "Ormosils of High Hardness," in: **Better Ceramics Through Chemistry VI**, eds. A.K. Cheetham, C.J. Brinker, M.L. Mecartney, C. Sanchez, Elsevier, New York, p. 397 (1994).

Xu, Y., Cheng, C.J., Mackenzie, J.D., "Electrically Ferroelectric-Like Properties of Amorphous Thin Films of Ferroelectric Oxides Prepared by the Sol-Gel Technique," Ceramic Transactions **55**, 215-222 (1995), Sol-Gel Sci. and Tech., eds, E.J.A. Pope, S. Sakka, L.C. Klein.

Lou, Y., Xu, Y., Mackenzie, J.D., "Multilayer Epitaxial $nX(SrTiO_3/PbTiO_3)$ Thin Films and Their Properties Prepared by the Sol-Gel Technique," Ceramic Transactions **55**, 207-213 (1995).

Wu, Q., Xu, Y., Park, S.S., Bescher, E.P., Mackenzie, J.D., "Optical Properties of Amorphous Multilayer Thin Films," Ceramic Transactions, **55**, 235-241 (1995).

Cheng, C.H., Xu, Y. and Mackenzie, J.D., "Optical Properties of Epitaxial Fe-Doped $KNbO_3$ Thin Film via Sol-Gel Method," Ceramic Transactions **55**, 243-250 (1995), Sol-Gel Science and Technology., eds. E.J.A. Pope, S. Sakka, L.C. Klein.

Mackenzie, J.D., "Hybrid Organic-Inorganic Materials," in: **Hybrid Organic Inorganic Composites**," Ed. J.E. Mark, C.Y.C. Lee, P.A. Bianconi, ACS Symp. 585 (1995).

Park, S.S., Mackenzie, J.D., "Sol-Gel Tin Oxide Thin Films," Thin Solid Films **15**[*28*] 268-273 (1995).

Park, S.S., Zheng, H.X., Mackenzie, J.D., "Sol-Gel Derived Antimony-Doped Tin Oxide Coatings on Ceramic Cloths," Materials Letters **22**[*3-4*], 175-180 (1995).

Park, S.S., Mackenzie, J.D., "Microstructure Effects in Multidipped Tin Oxide Films," J. Amer. Ceramic Society **78**[*10*], 2669-2672 (1995).

Iwamoto, T., Mackenzie, J.D., "Ormosil, Coatings of High Hardness," J. Materials Science **30**[*10*], 2566-2570 (1995).

Iwamoto, T., Mackenzie, J.D., "Hard Ormosils Prepared with Ultrasonic Irradiation," J. Sol-Gel Science and Technology 4[2], 141-150 (1995).

Bescher, E.P., Mackenzie, J.D., "Organic-Inorganic Composites with Optical Properties in the Near-Infrared," Ceramic Transactions **55**, 275-281 (1995), J. Sol-Gel Science and Technology, eds. E.J.A. Pope, S. Sakka, L.C. Klein.

Hoshino, Y., Mackenzie, J.D., "Viscosity and Structure of Ormosil Solutions," J. Sol-Gel Science and Technology **5**[2], 83-92 (1995).

Mackenzie, J.D., "Present and Future Directions in Sol-Gel Science and Technology," Ceramic Transactions **55**, 25-31 (1995), eds. E.J.A. Pope, S. Sakka, L.C. Klein, Amer. Ceramic Society, Ohio.

Huang, Q., Mackenzie, J.D., "A Study on Reinforcement of Rubber-Like Ormosils," Ceramic Transactions **55**, 291-298 (1995), eds., E.J.A. Pope, S. Sakka, L.C. Klein, Amer. Ceramic Society, Ohio.

Park, S.S., Mackenzie, J.D., "Thickness and Microstructure Effects on Alcohol Sensing of Tin Oxide Thin Films," Thin Solid Films **274**, 154-159 (1996).

Hong, E., Bescher, E., Garcia, Lynne, Mackenzie, J.D., "Detection of Crysptosporidium Parvum in Antibody-Doped Gels," in: **Better Ceramics Through Chemistry VII**, ed. C. Sanchez, MRS Symp. Proc. **435**, 449-454 (1996).

Bescher, Eric Pascal, Hong, Edward, Xu, Yuhuan, Mackenzie, J.D., "Dipolar Organic/Ferroelectric Oxide Hybrids, in: **Better Ceramics Through Chemistry VII**, ed. C. Sanchez, MRS Symp. Proc. **435**, 605-609 (1996).

Mackenzie, J.D., Huang, Q., Rubio-Alonso, F., Kramer, S.J., "Effects of Temperature on Properties of Ormosils," MRS Symp. Proc. **435**, 229-236 (1996).

Kramer, S.J., Rubio-Alonso, F., Mackenzie, J.D., "Organically Modified Silicate Aerogels, Aeromosils," MRS Symp. Proc. **435**, 295-300 (1996).

Tsuru, K., Osaka, A., Iwamoto, T., Mackenzie, J.D., "Synthesis of Bioactive Ormosils by the Sol-Gel Method," MRS Symp. Proc. **435**, 403-406 (1996).

Park, S.S., Mackenzie, J.D., Li, C.Y., Peyghambarian, N., "Fiber Optic Sensing of Cyanides in Solutions," MRS Symp. Proc. **435**, 667-672 (1996).

Mackenzie, J.D., "The Future of Glass Research," Glass Tech. **37**, 181-184 (1991).

Xu, Y., Cheng, C.H., Mackenzie, J.D., "Epitaxial $KNbO_3$ and Fe-Doped $KNbO_3$ Thin Films Prepared by the Sol-Gel Technique," MRS Symp. Proc. **433**, 401-406 (1996).

Mackenzie, J.D., Huang, Q., Iwamoto, T., "Mechanical Properties of Ormosils," J. Sol-Gel Science and Technology **7**, 151-161 (1996).

Mackenzie, J.D., "Sol-Gel Processing of Inorganic-Organic Hybrid Materials," Norbert Kreidl Symp., Eds. W. Holand, V. Reinberger, Glastech. Berichte, **70C**, 181-188 (1997).

Bescher, E.P., Xu, Y., Mackenzie, J.D., "Ferroelectric-Glass Composites," SPIE Proc. **3136**, 397-406 (1997).

Dunn, B.S., Mackenzie, J.D., Pope, E.J.A., Schmidt, H.K., Yamane, M., Eds. Sol-Gel Optics IV, SPIE Proc. (1997).

Inoue, H., Park, S.S., Bescher, E., Mackenzie, J.D., "Detection of Gaseous Molecules by Capacitance Variation in Organically Modified Silicate (Ormosil) Films," J. Sol-Gel Science and Technology **11**, 67-86 (1997).

Xu, Y., Cheng, C.H., Lou, Y., Mackenzie, J.D., "Epitaxial Ferroelectric Thin Films by the Sol-Gel Technique," Ferroelectrics **195**, 283-288 (1997).

Ho, I.C., Xu, Y., Mackenzie, J.D., "Electrical and Optical Properties of MgO Thin Film Prepared by Sol-Gel Technique," J. Sol-Gel Science and Technology **9**, 295-301 (1997).

Mackenzie, J.D., Xu, Y., "Ferroelectric Materials by the Sol-Gel Method," J. Sol-Gel Science and Technology 8, 673-679 (1997).

Mackenzie, J.D., Bescher, E., "Formation and Properties of Ultrafine Particles in Glass," Proc. XVII International Congress on Glass, San Francisco, July 5-10, 1998, accepted for Publication.

Mackenzie, J.D., Bescher, E., "Obstacles to Applications of Sol-Gel Science," Proc. XVIII International Congress on Glass, San Francisco, July 5-10, 1998, accepted for publication.

Mackenzie, J.D., Bescher, E., "Structures, Properties and Applications of Ormosils," J. Sol-Gel Science and Technology (1998), accepted for publication.

Xu, Y., Cheng, C.H., Mackenzie, J.D., "Microstructure in Heteroepitaxial $KNbO_3$ Thin Films," J. Phys. Soc. Korea (1998), accepted for publication.

Zhu, D., Li, Q., Mo, Dang, Xu, Y., Mackenzie, J.D., "Optical Properties of Lead Lanthanum Zirconate Titanate Ferroelectric Thin Films, Thin Solid Films, 1998, accepted for publication.

5. Student Training

During this grant period, the following graduate students have received their M.S. and Ph.D. degrees through the support of this grant.

(a) M.S. Degree Recipients

Justine Y. Tseng
Eva M. Wong
Giovanni Minervi
Yudan Lou
Stephen J. Kramer
Soon-Ku Yuh
John Gonzalez
Amy Roschelle
Tammy Chau
Yasukazu Hoshino
Brady Shih
Charles Q. Wu
Phillip Wong

(b) *Ph.D. Degree Recipients*

Kevin J. Thorne
C.-Y. Li
S.S. Park
Yuhuan Xu
Ken C.H. Cheng
Eric P. Bescher

6. Postdoctoral Scholars and Visitors

Dr. Fausto Alonso (Spain)
Dr. I.C. Ho (Taiwan)
Dr. H. Unuma (Japan)
Ms. Yu Ling (PRC)
Dr. Q. Huang
Dr. Yuhuan Xu
Dr. S.S. Park (Korea)
Dr. A. Matucci (Italy)
Dr. F. del Monte (Spain)
Dr. H. Inoue (Japan)

7. Professional Activities and Recognition

Professor J.D. Mackenzie was organizer and chair of Sol-Gel Optics III and IV in 1994 and 1997, respectively for SPIE. These international conferences attract an audience of 200-300 people and are now well recognized by scientists and engineers involved in optical materials. Professor Mackenzie continued to be an active member of the International Advisory Committee which organizes the Workshop on Sol-Gel Science and Technology. The last two workshops were in Portugal (1995) and in the Untied Kingdom (1997). Professor Mackenzie was named Cecil and Ida Green Honors Professor by Texas Christian University in May, 1994, the Samuel S. Scholes Lecturer by Alfred University, Alfred, New York in March, 1995 and the W.E.S. Turner Lecturer by Sheffield University, Sheffield, U.K. in May, 1996.

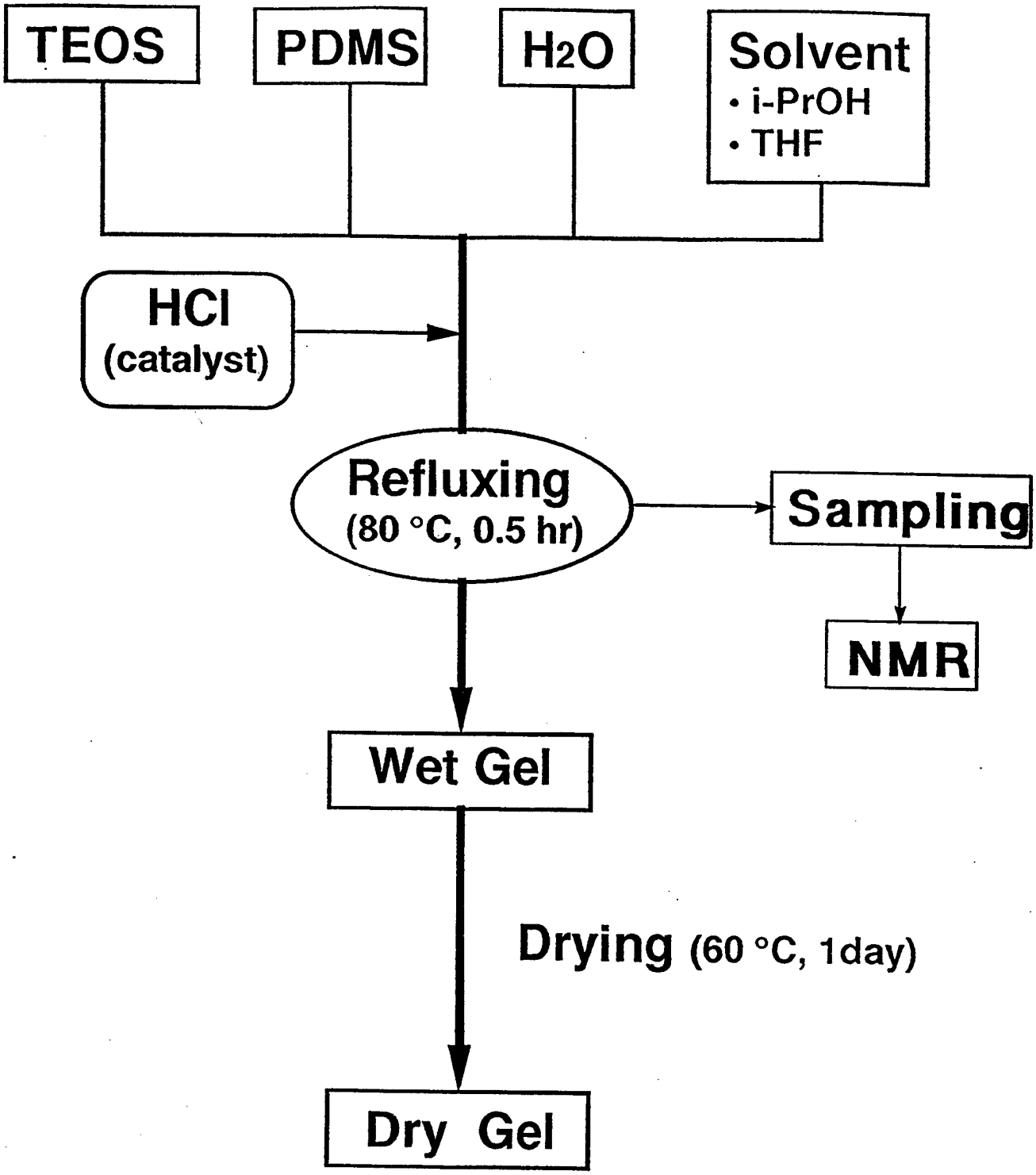

Figure 1 Flow sheet of preparing ORMOSILs through refluxing process

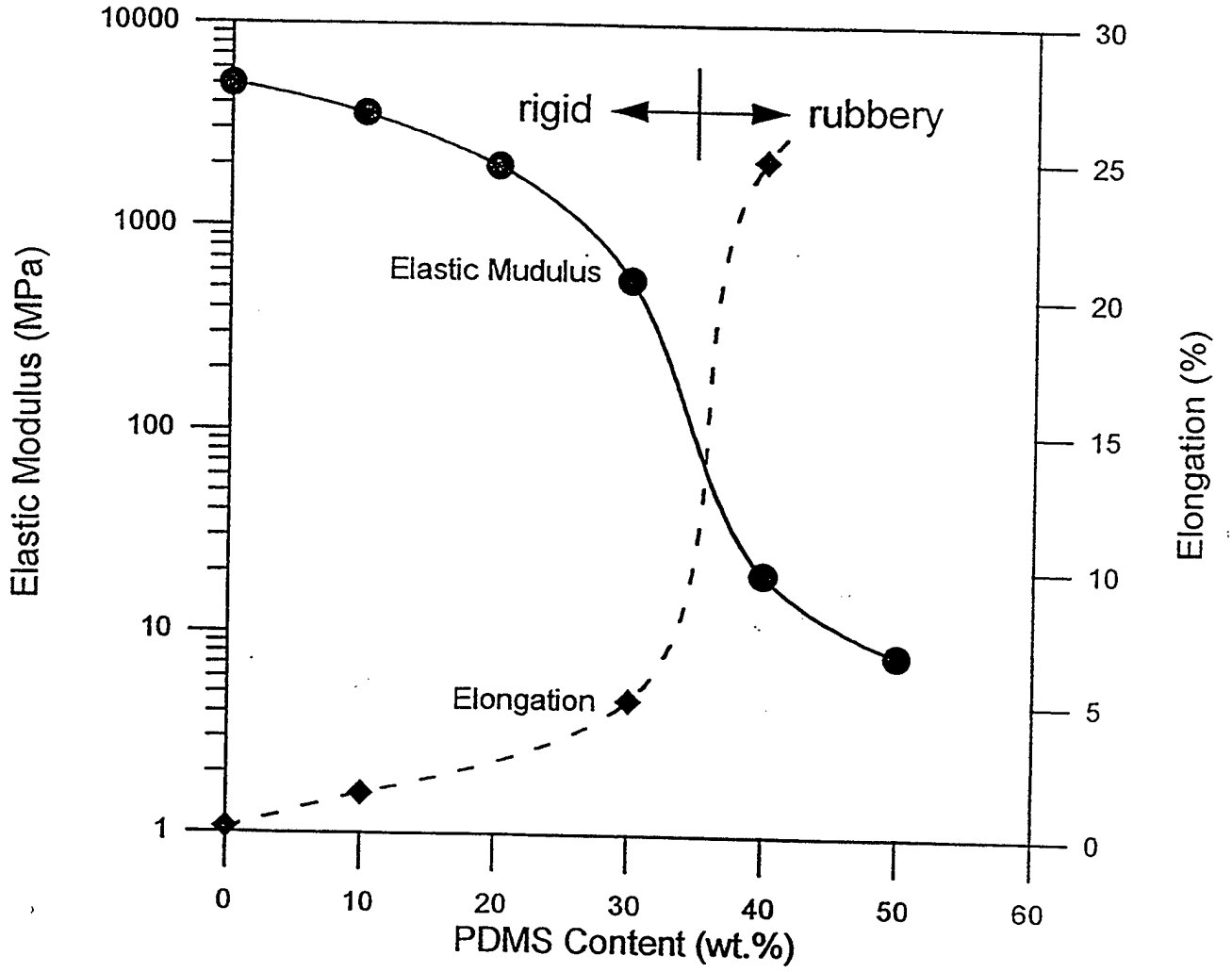

Figure 2 Variation of mechanical properties of Ormosils as a function of PDMS content

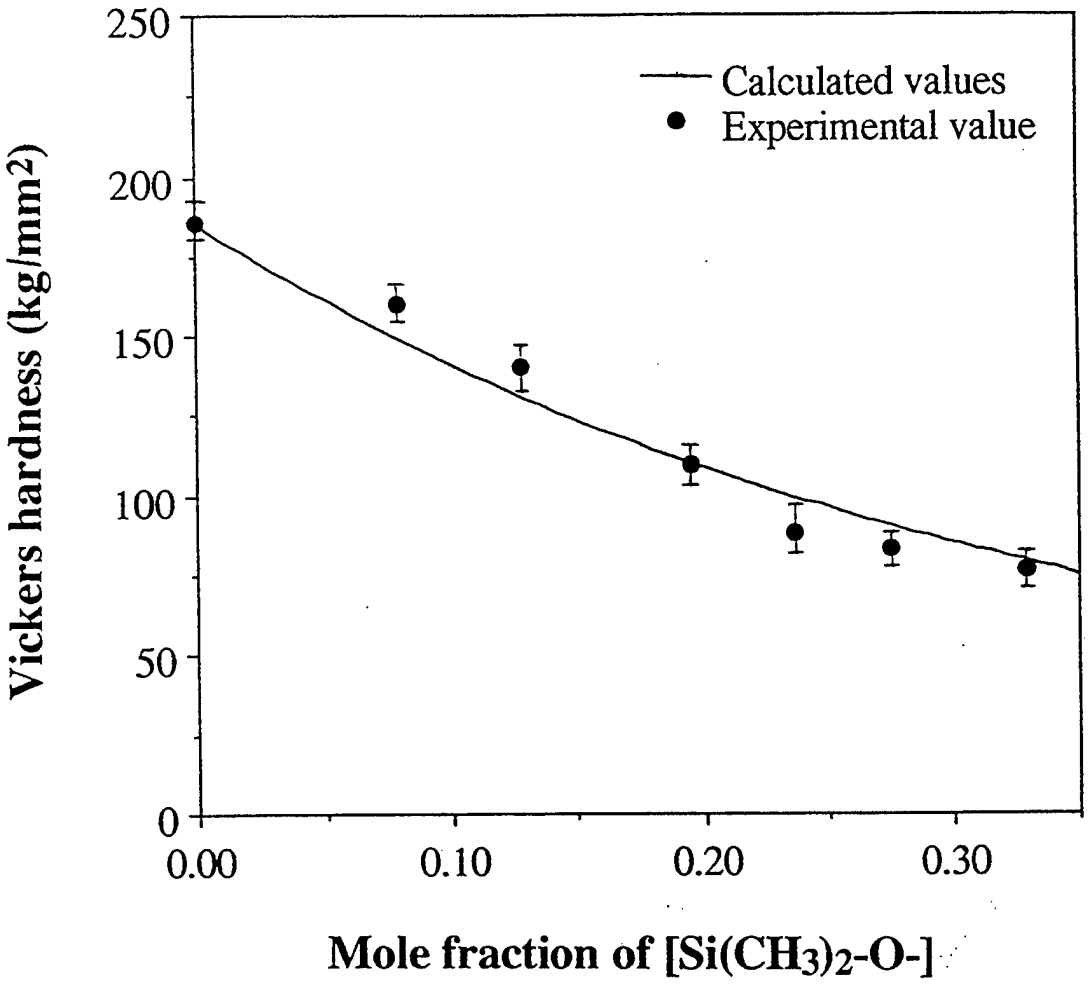

Figure 3 Vickers hardnesses of the TEOS/PDMS system hard ormosils

Figure 4 Modification of the Random Network Structure of SiO_2 by PDMS

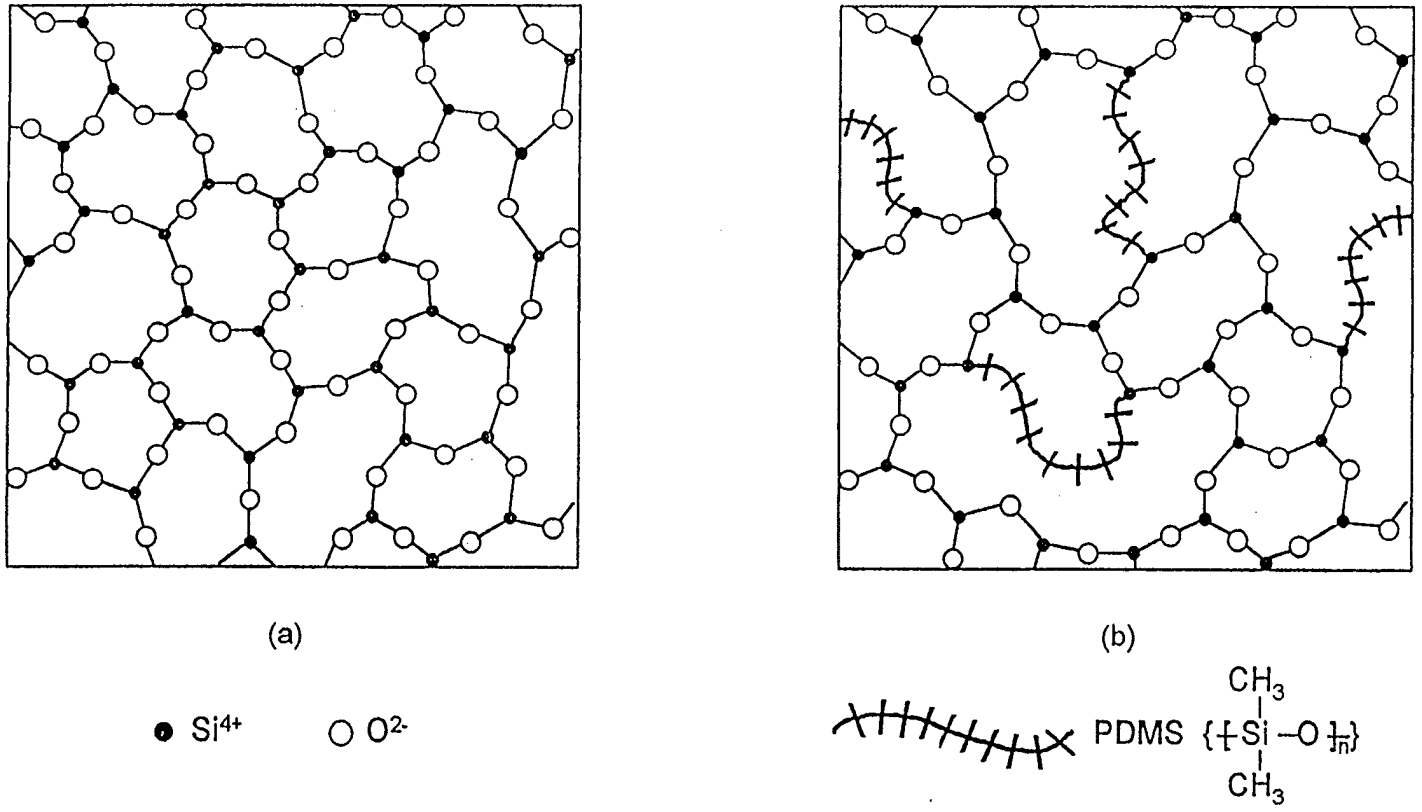

Figure 5 Rubbery Ormosil from High Concentrations of PDMS in SiO_2

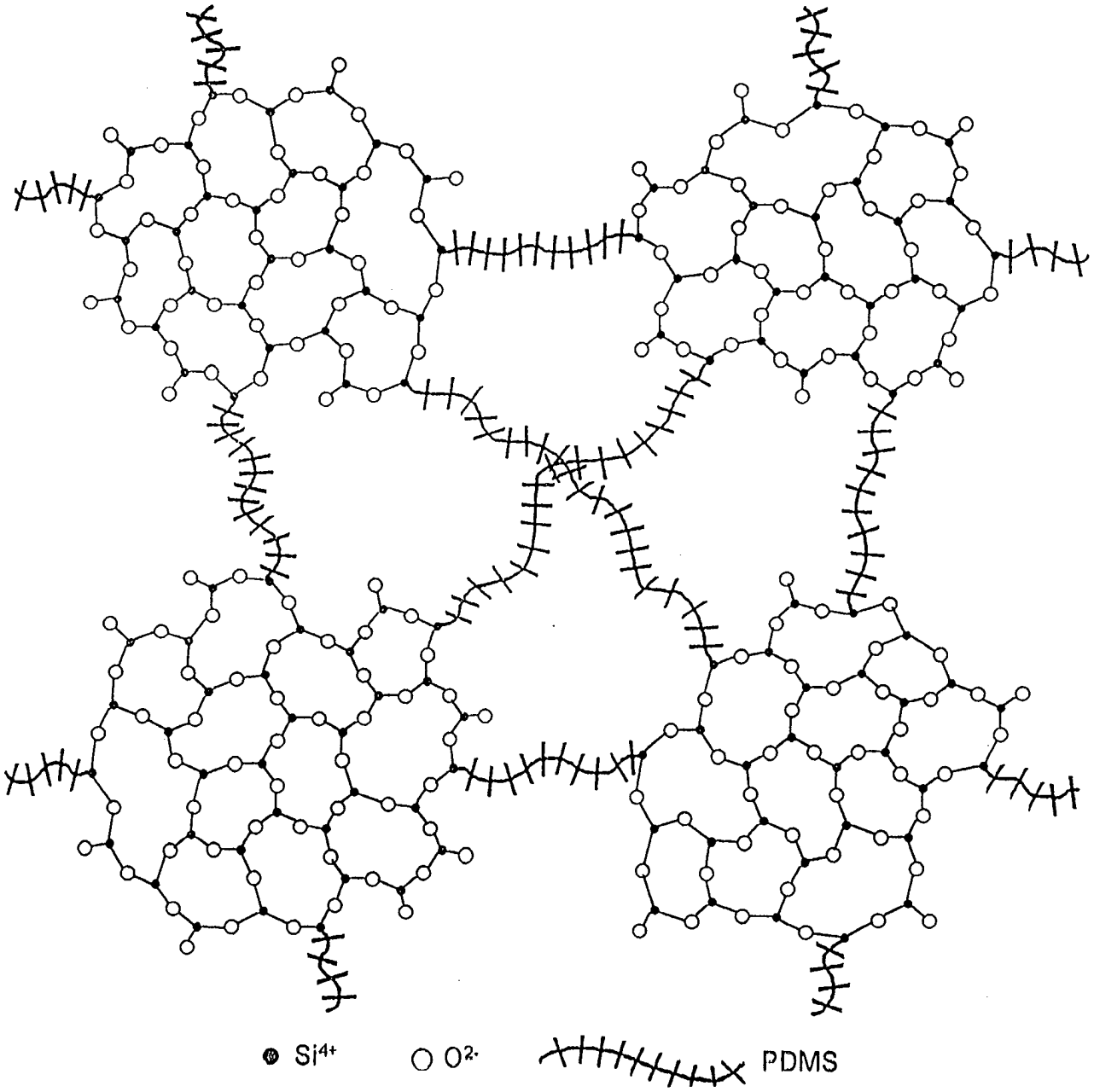

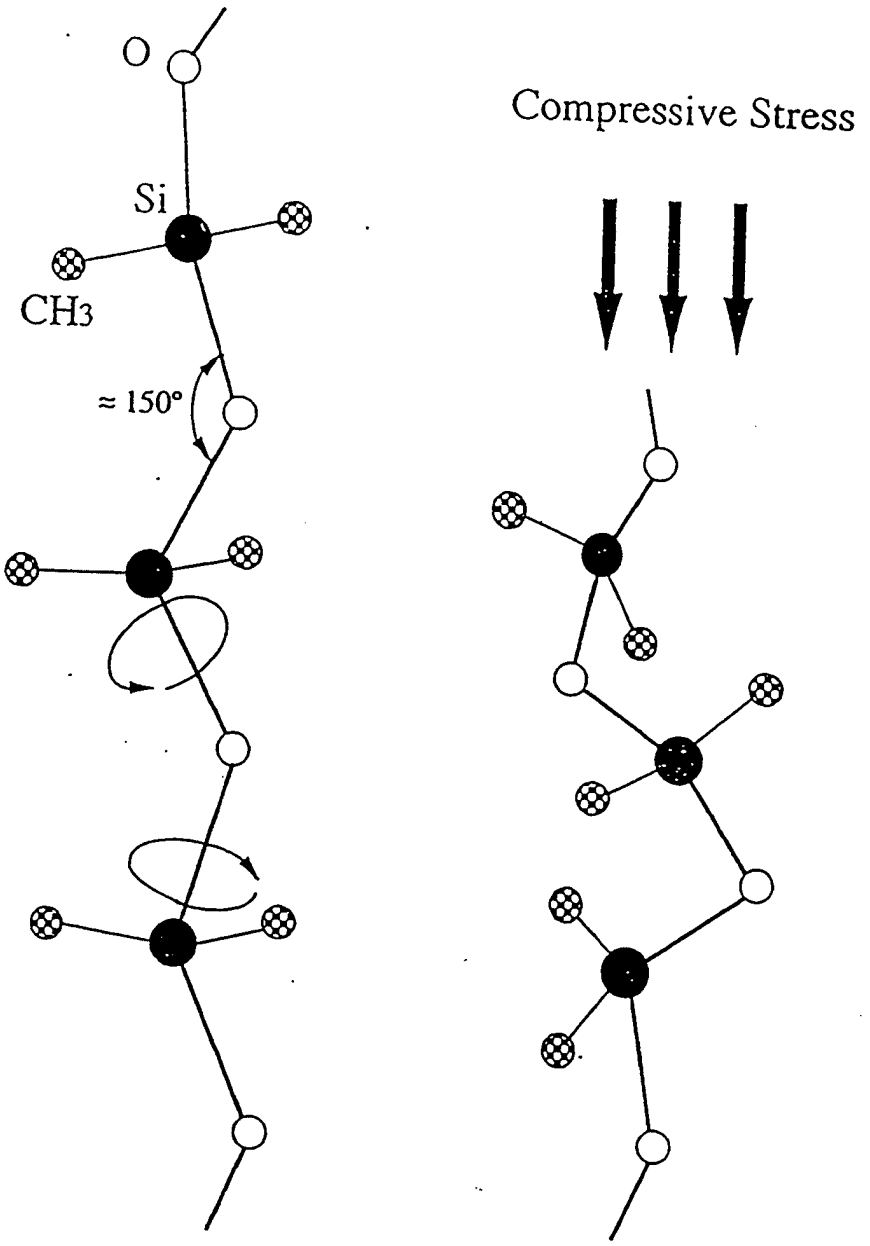

Chain can be shortened by rotation around Si-O-Si

Figure 6 Coiling of PDMS chains

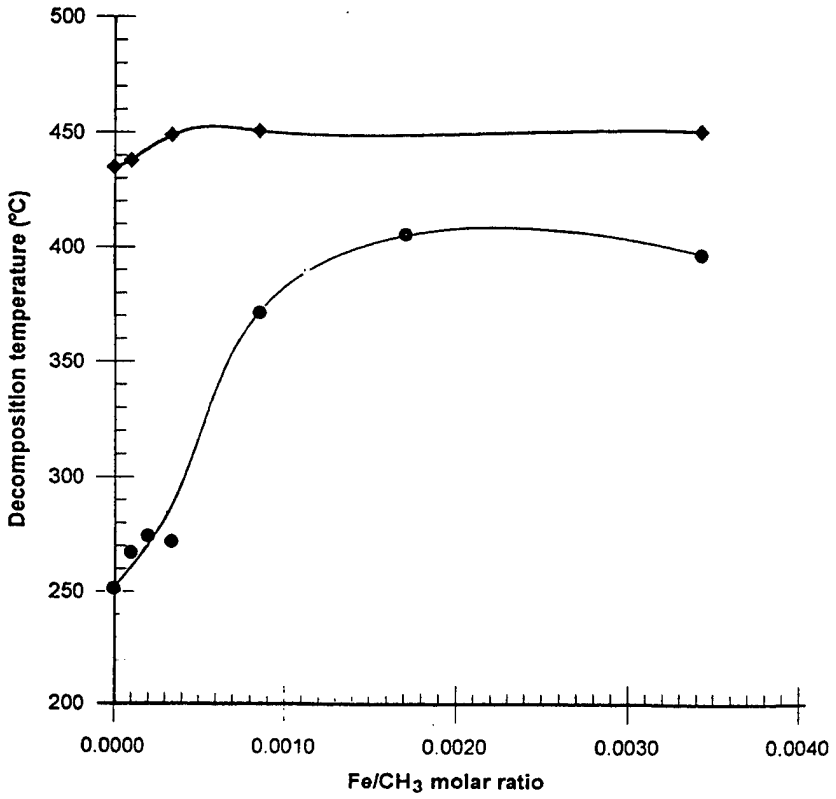

Figure 7 Effect of iron on thermal decomposition temperature, by TGA, of ORMOSILs in air (bottom curve) and in nitrogen

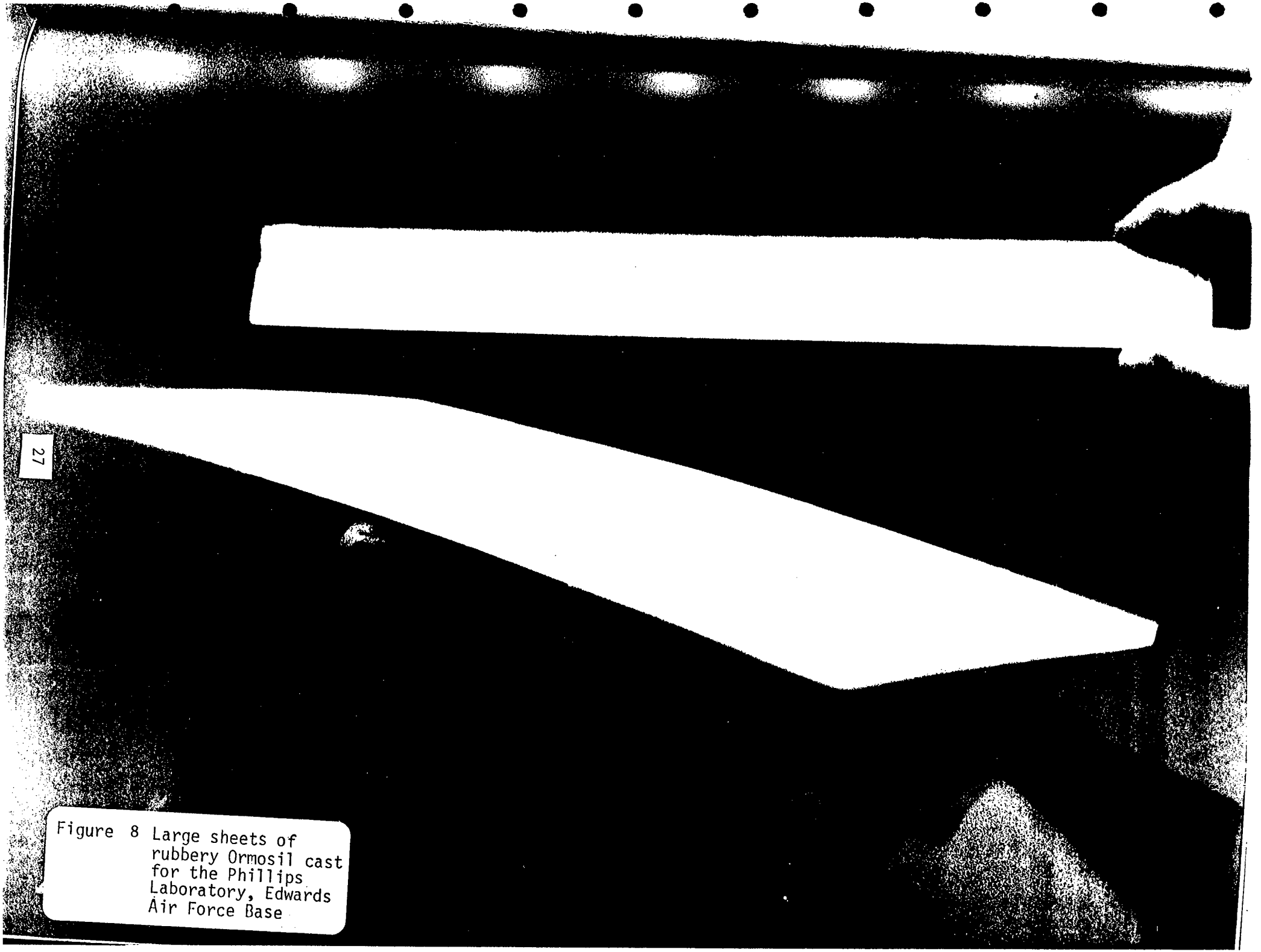

Figure 8 Large sheets of rubbery Ormosil cast for the Phillips Laboratory, Edwards Air Force Base

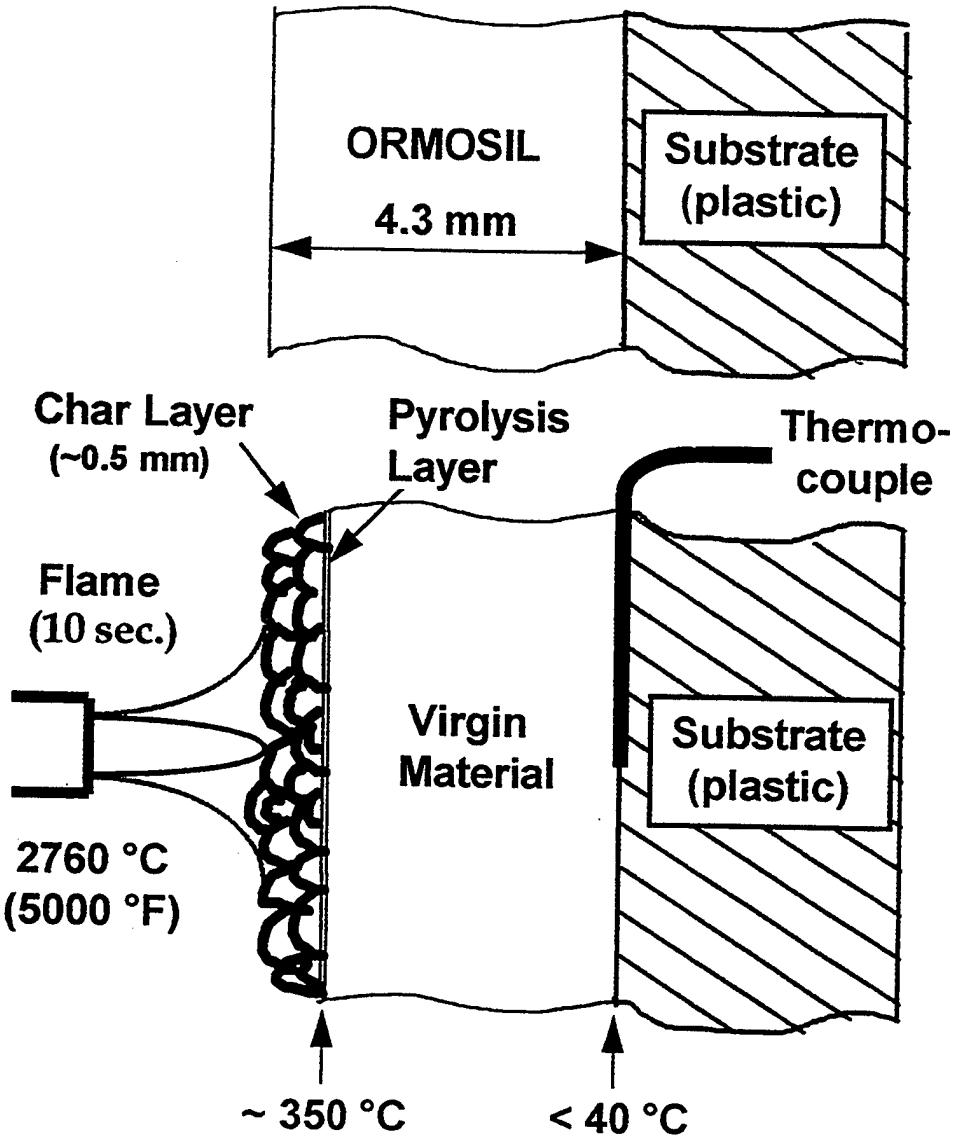

Figure 9 Insulating mechanism of ORMOSIL against extremely high temperature flame

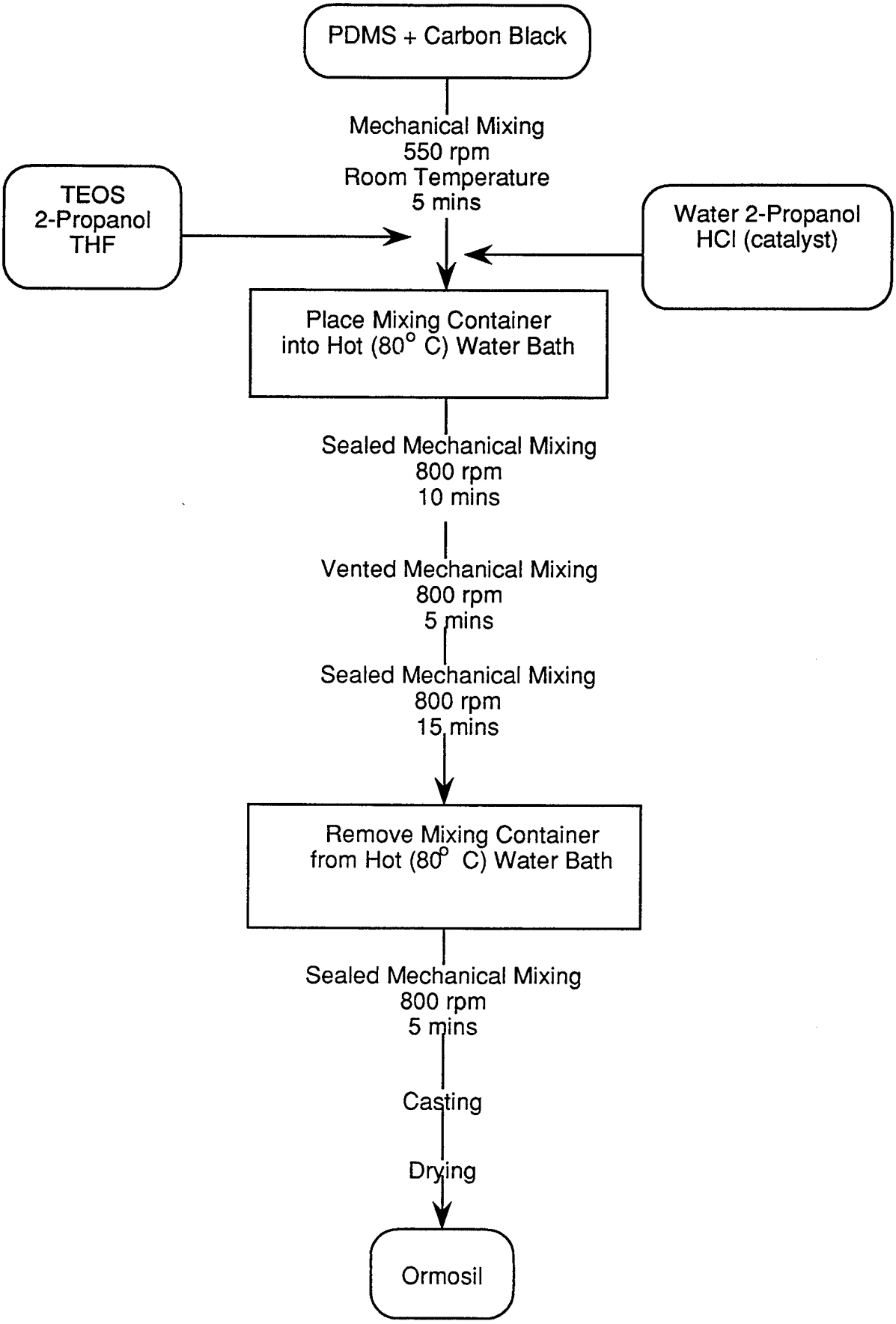

Figure 10 Flow chart for mechanical mixing

Tensile strengths of carbon black filled ORMOSILs as a function of percent loading

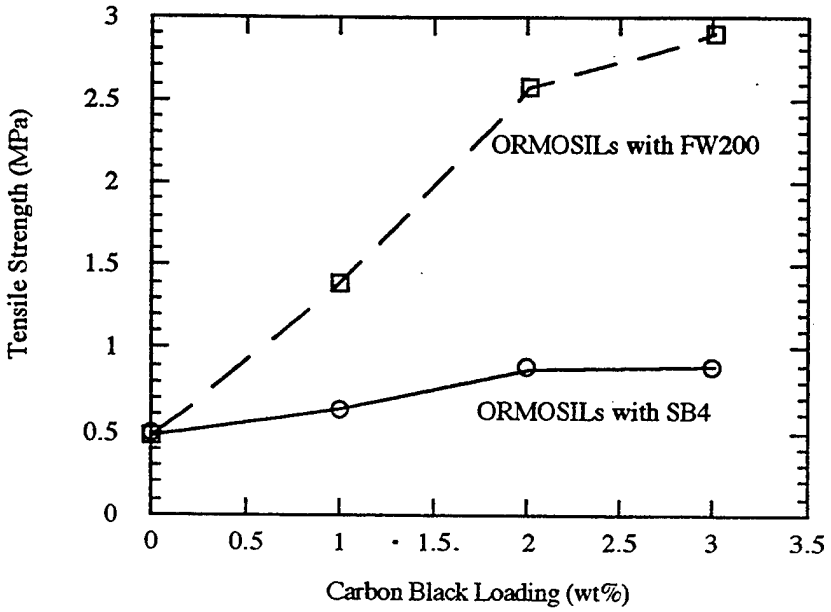

Figure 11

Resilience of carbon black filled ORMOSILs as a function of percent loading

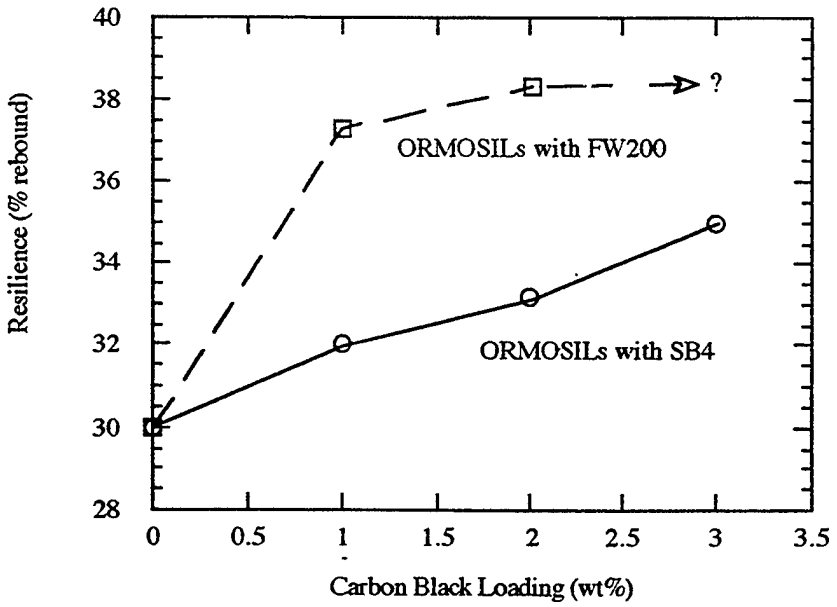

Figure 12

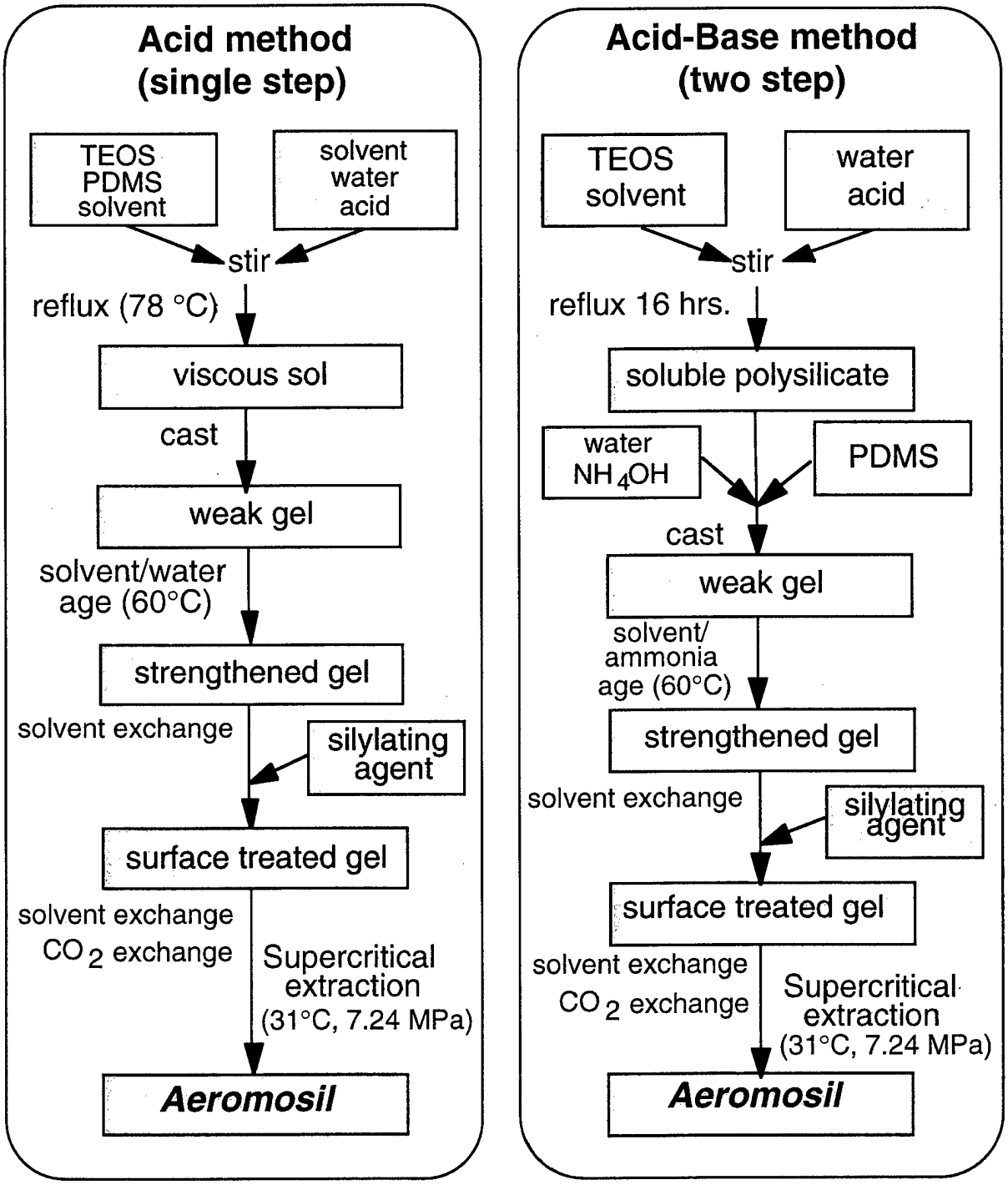

Figure 13 Flow chart schematic of acid and acid-base catalyzed Aeromosil formation

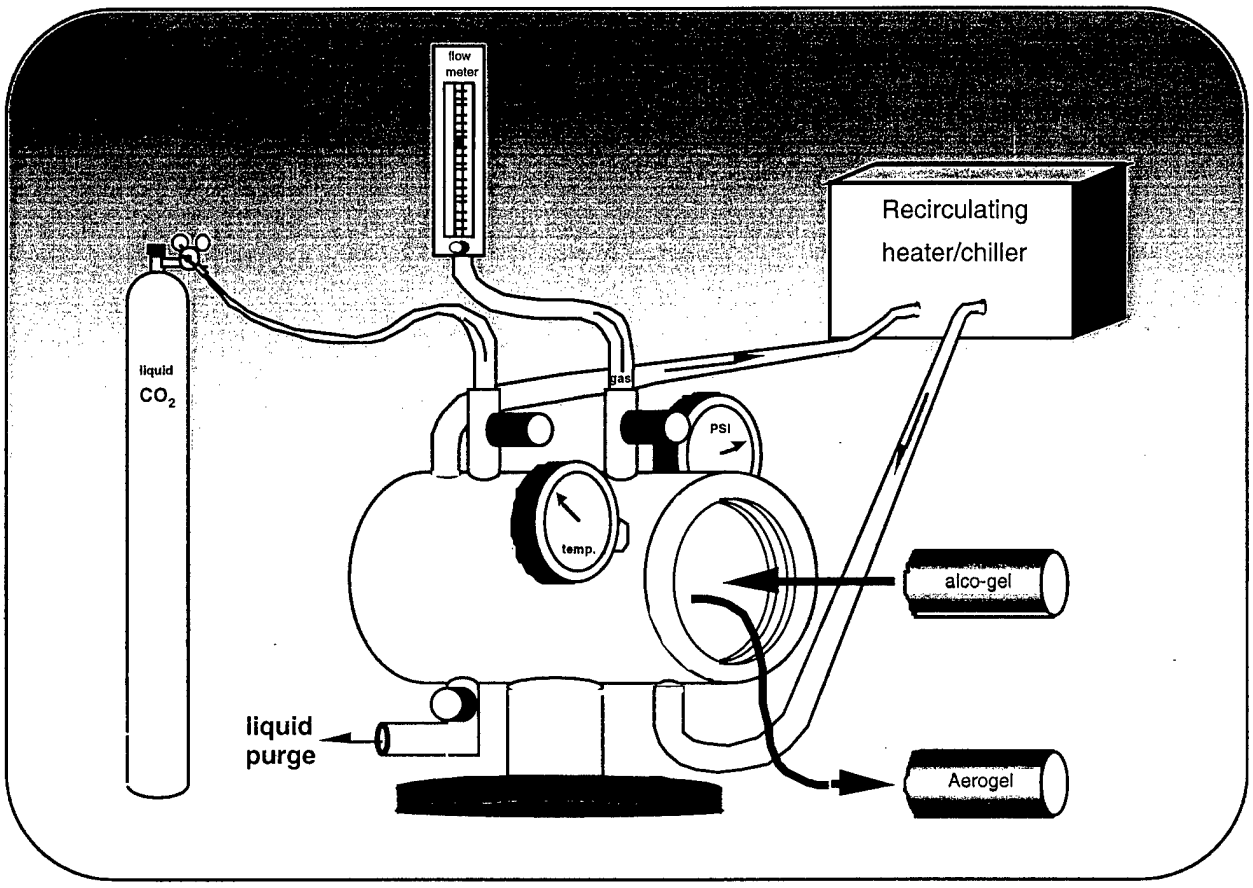

Figure 14 Schematic representation of a supercritcal drying apparatus used to make rubbery Aeromosils

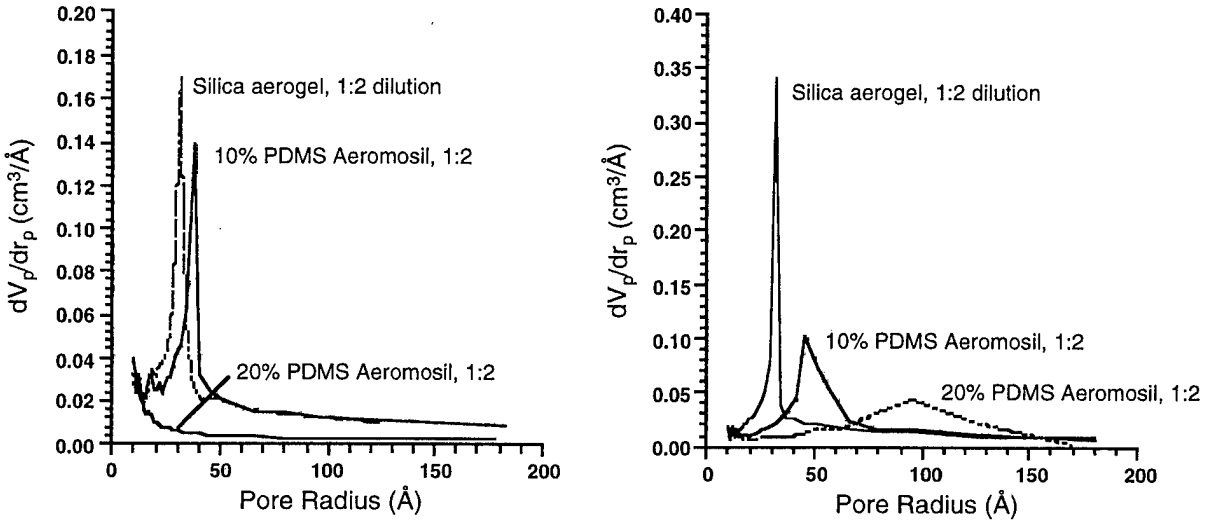

Figure 15 Pore size distributions for aerogels with varying concentrations of PDMS, a) acid catalyzed and b) acid/base catalyzed

Figure 16 Rubbery Behavior of Aeromosils

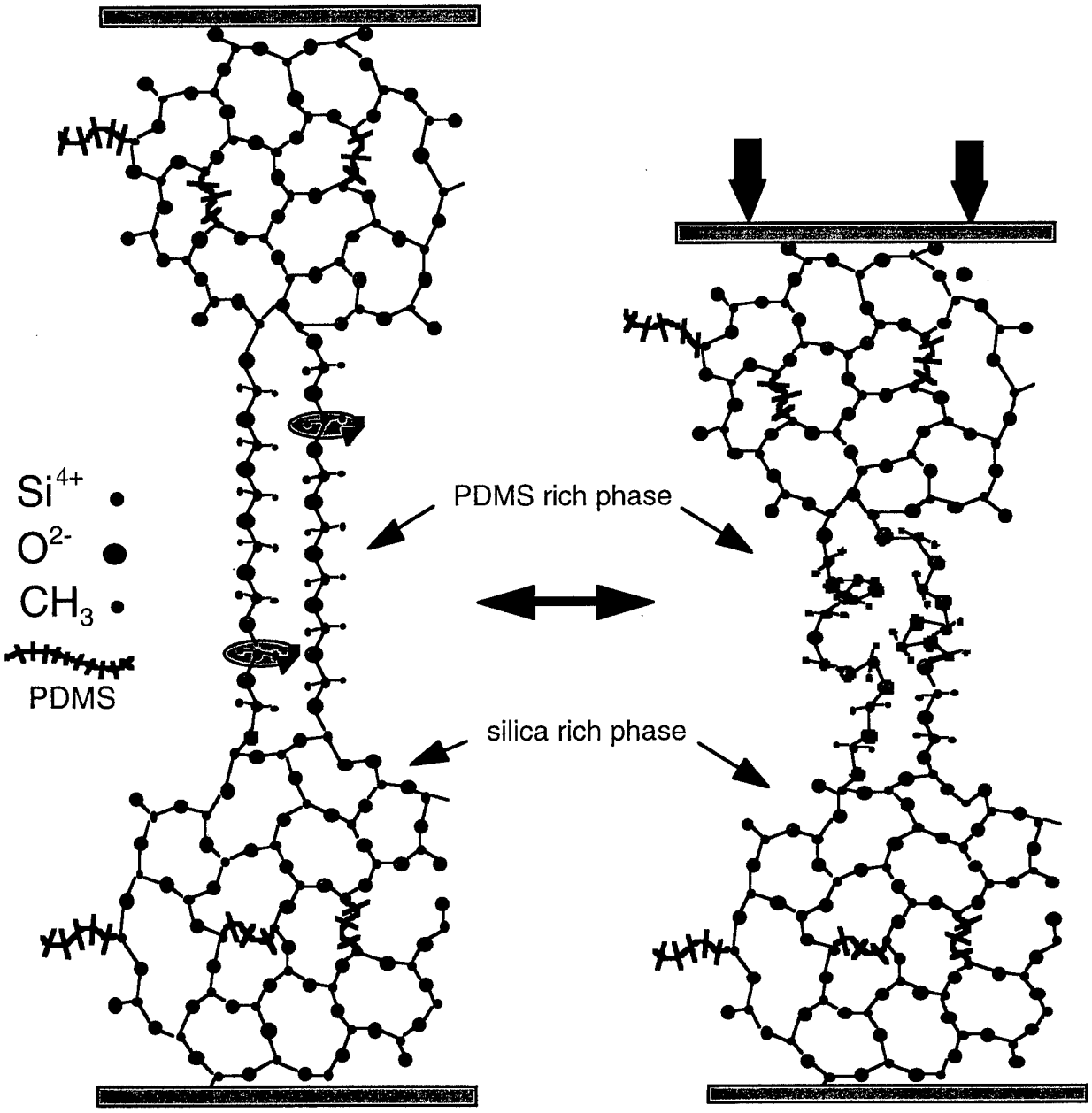

Figure 17 Model of rubbery behavior in Aeromosils based on preferential phase segregation of PDMS and silica rich phases

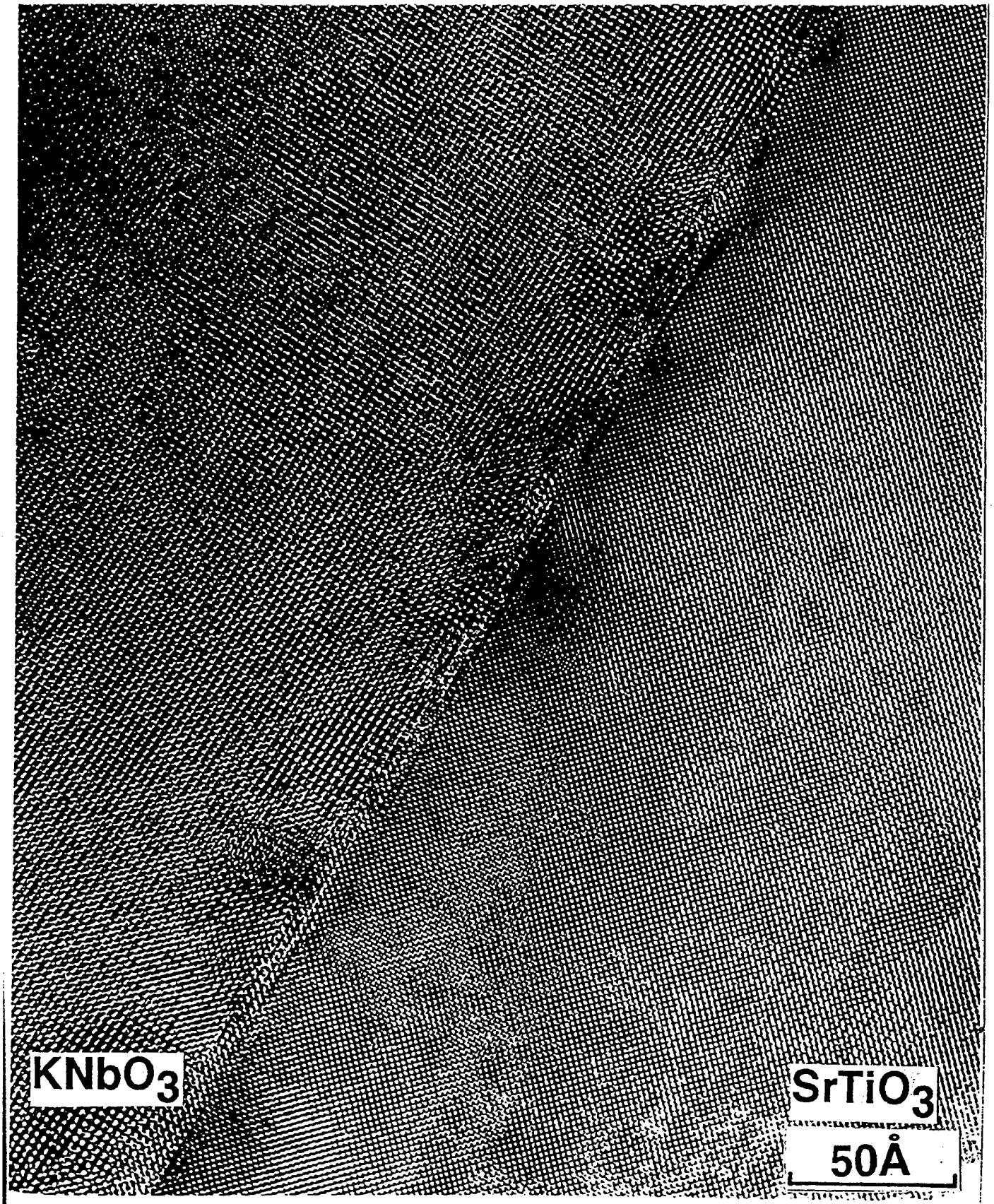

Figure 18 Lattice fringe image of epitaxial single crystal $KNbO_3$ film on $SrTiO_3$

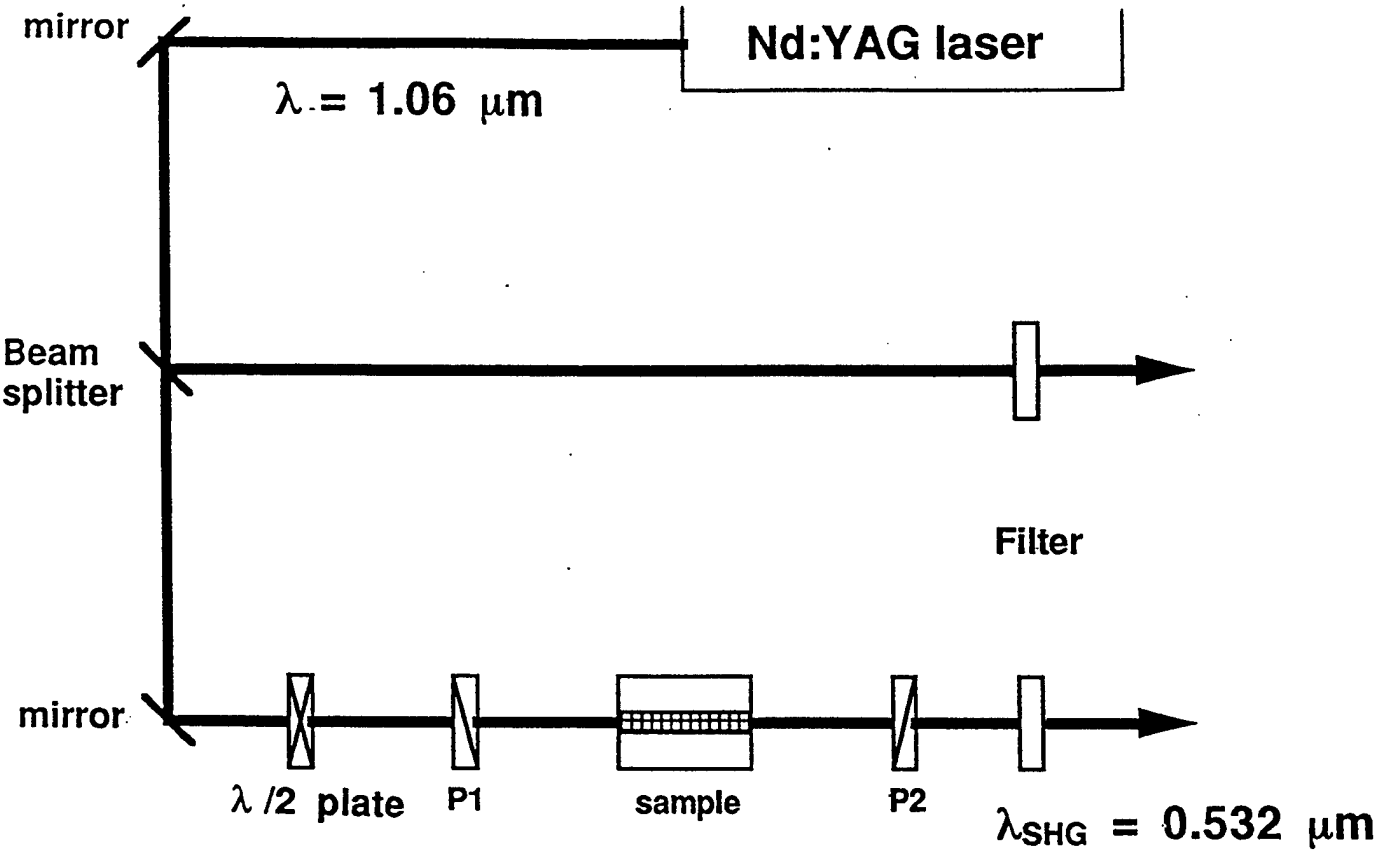

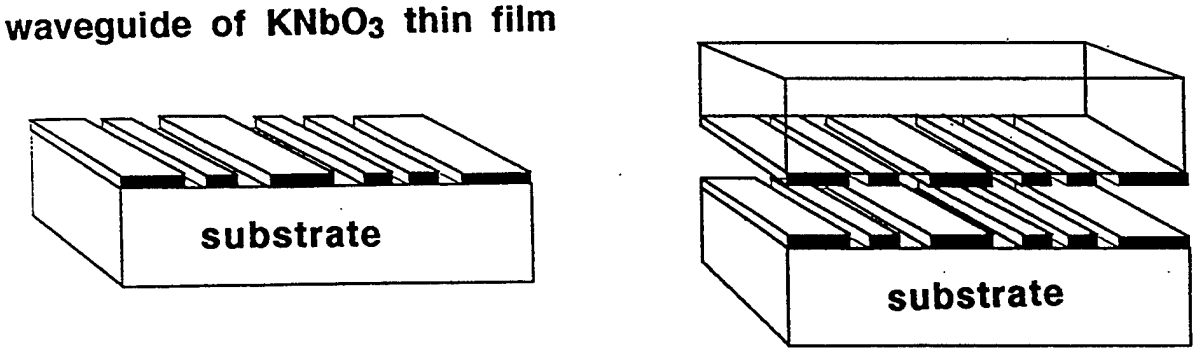

Figure 19 The experimental setup for the second harmonic generation and the waveguide pattern of the epitaxial $KNbO_3$ thin films

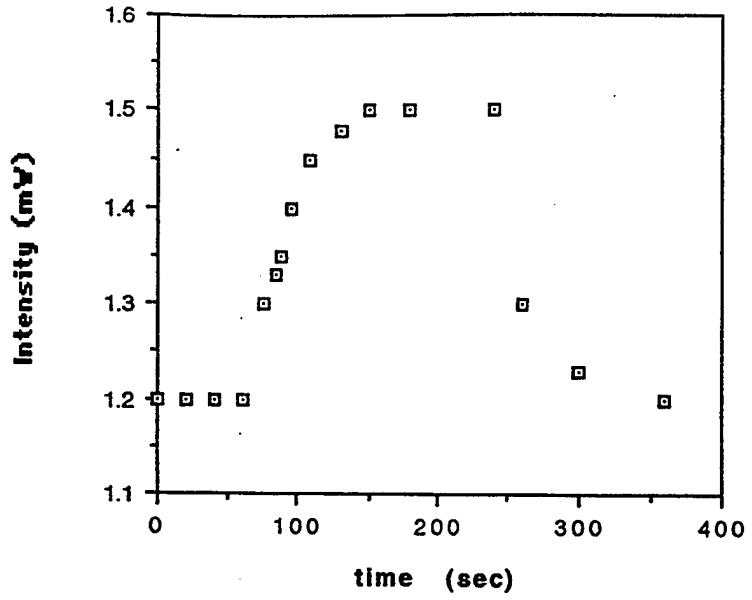

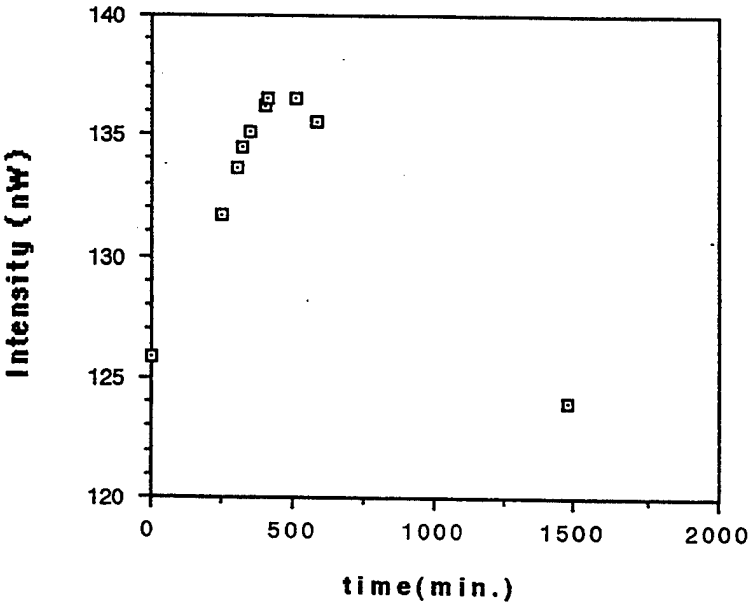

Figure 20 Intensity amplification of the laser light by using (a) $\lambda = 0.532$ μm, 1.2 W, (b) $\lambda = 0.633$ μm, 0.3 mW, in the Fe-doped $KNbO_3$ thin films by the two-wave mixing experiments

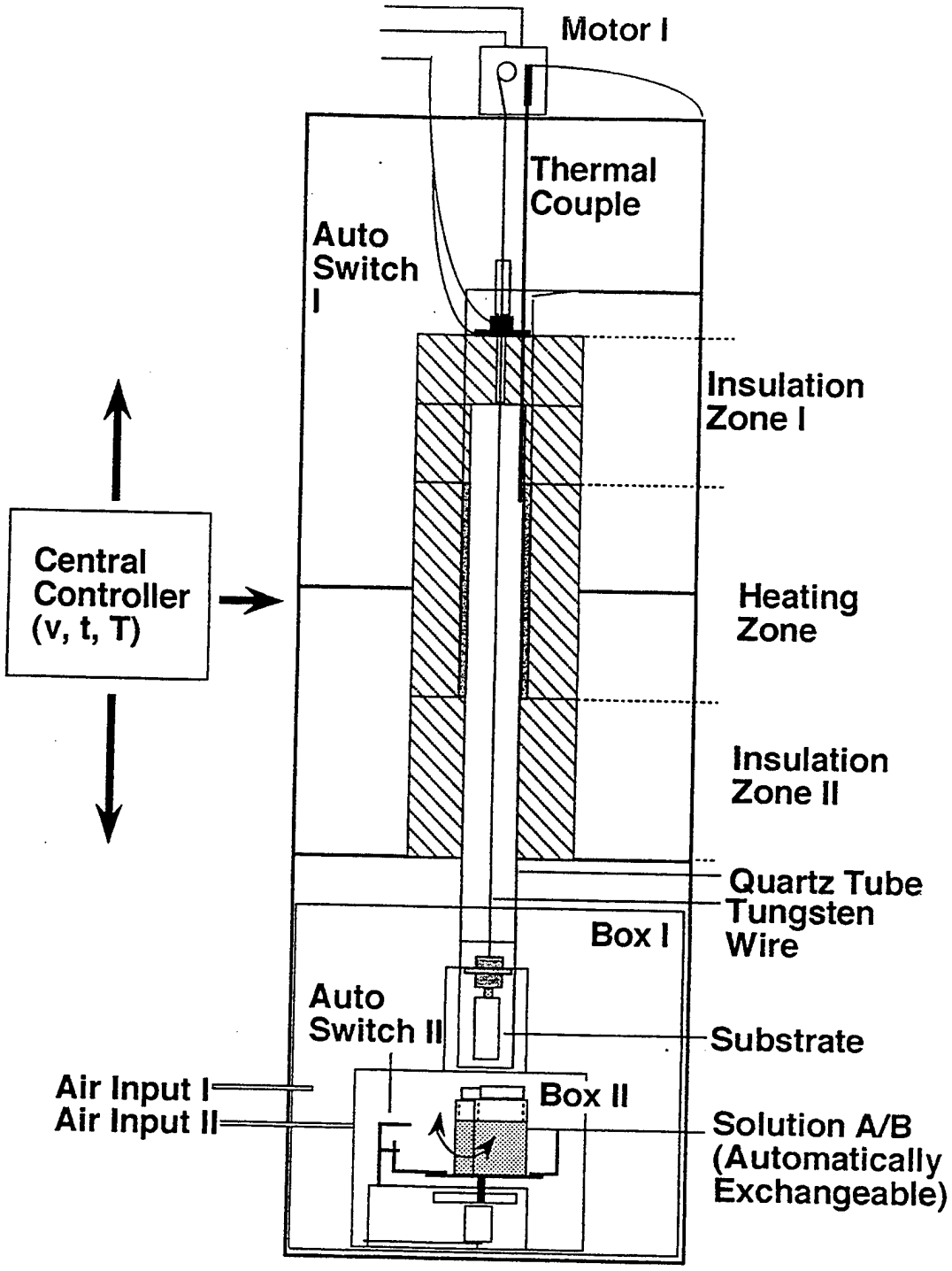

Figure 21 Schematic drawing of the automotic dip-coating and heating apparatus

SEM CHARACTERIZATION

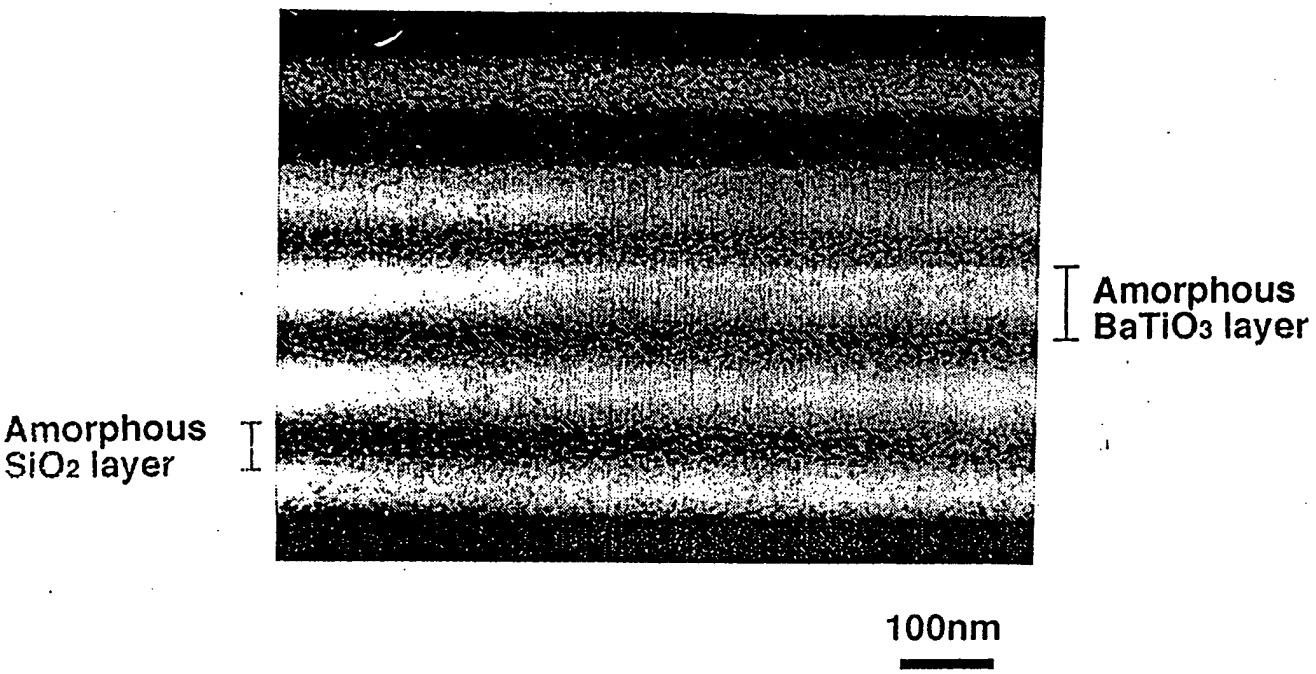

Figure 22 Electron micrograph of the cross-section through layers of amorphous $BaTiO_3/SiO_3$ films, where dark layers represent SiO_2 and white layers represent $BaTiO_3$ (deposited alternatingly from solutions of 0.25 M BaTi(OR)x and 0.87 M $Si(OC_2H_5)_x$ upon fused silica substrates and fires at 400°C

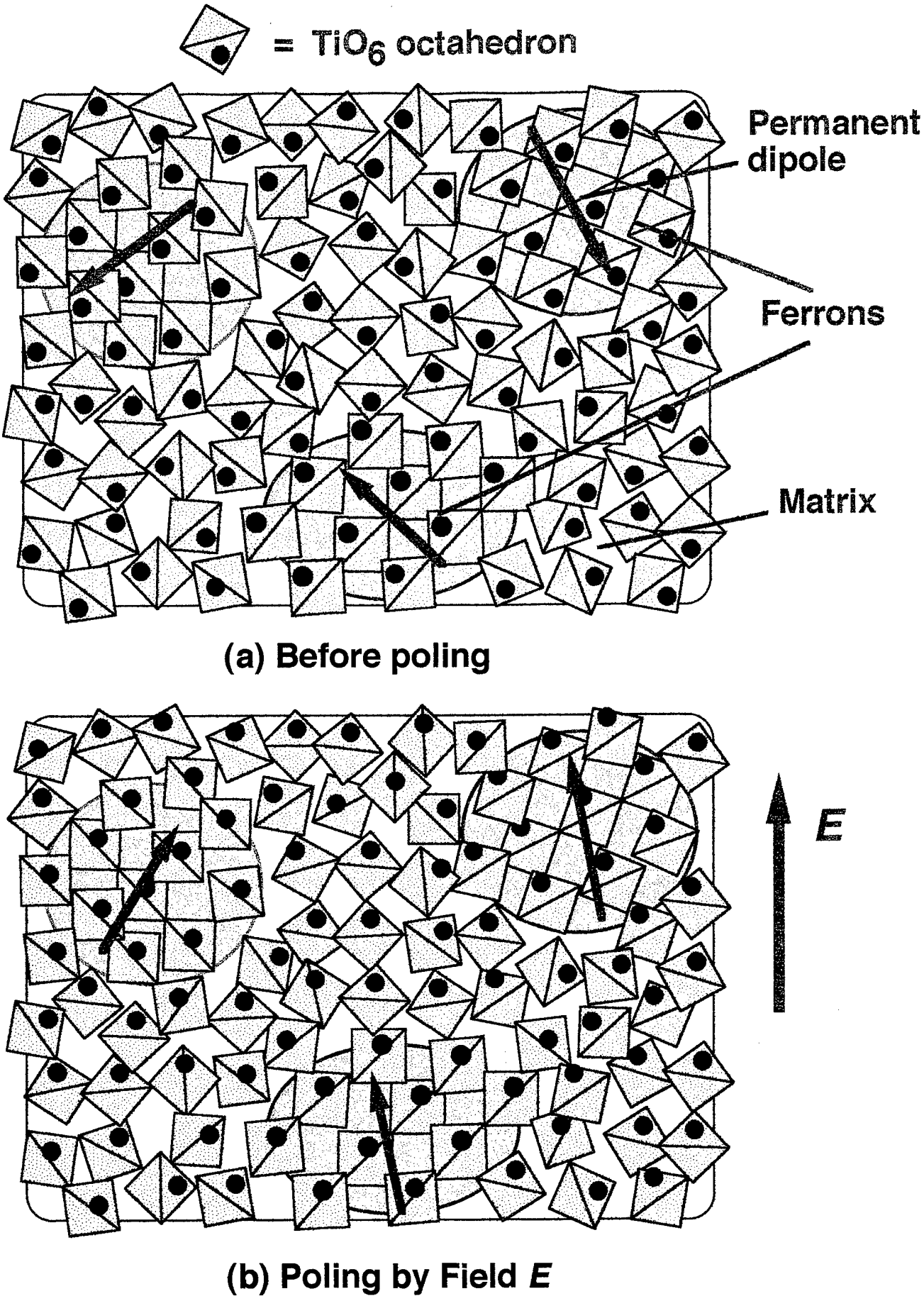

Figure 23 The "ferron" coupling model for oxide ferroelectrics

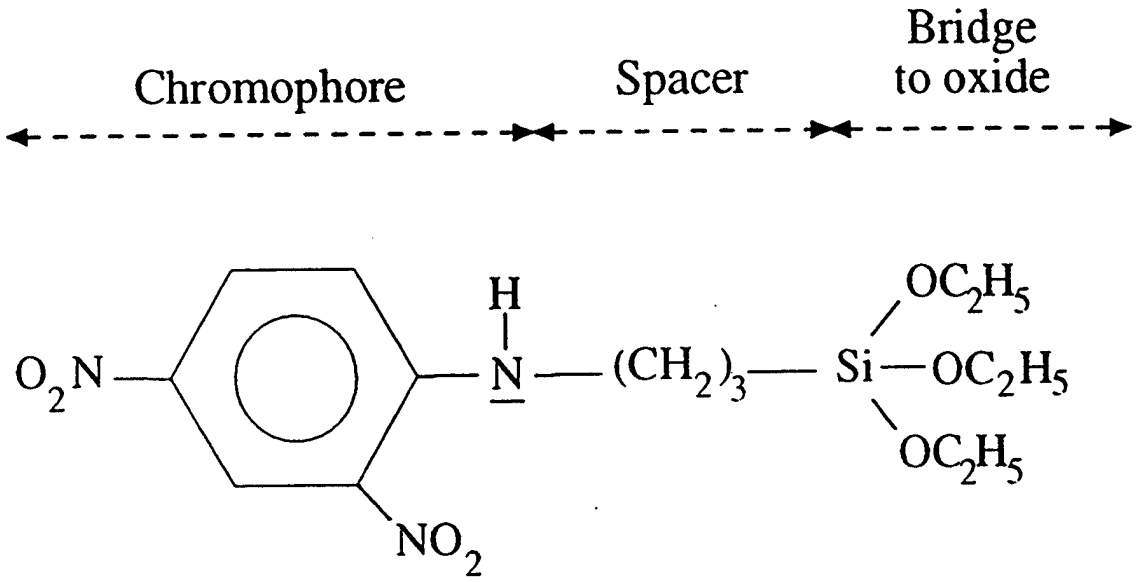

Figure 24 TDP: Triethoxy-silyldinitro-phenylamine

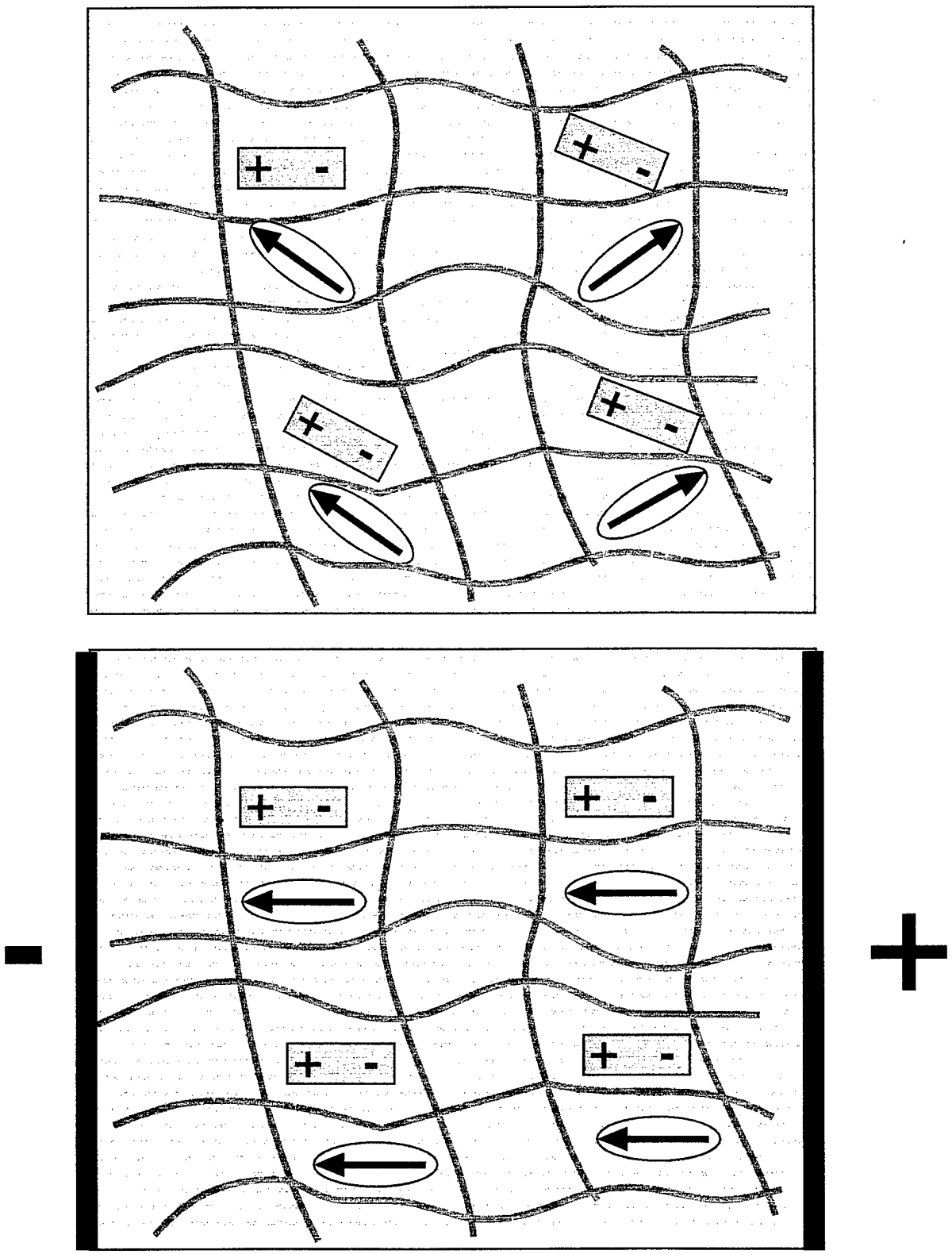

Figure 25 Electrical interactions of organic groups (arrow) and inorganic groups (+ -) in a gel matrix

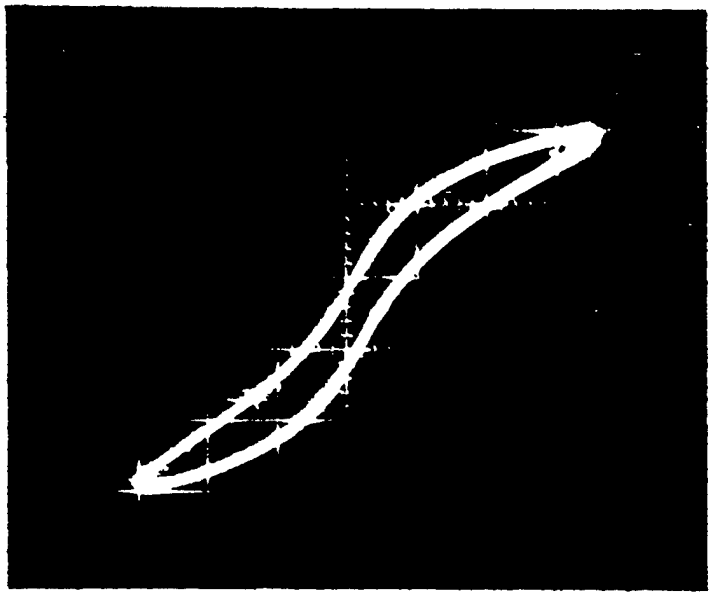

45 mol% TDP-45 mol% $LiNbO_3$-10mol% TEOS film
200°C/ 2hr

Figure 26 P-E Hysteresis loop in gel film

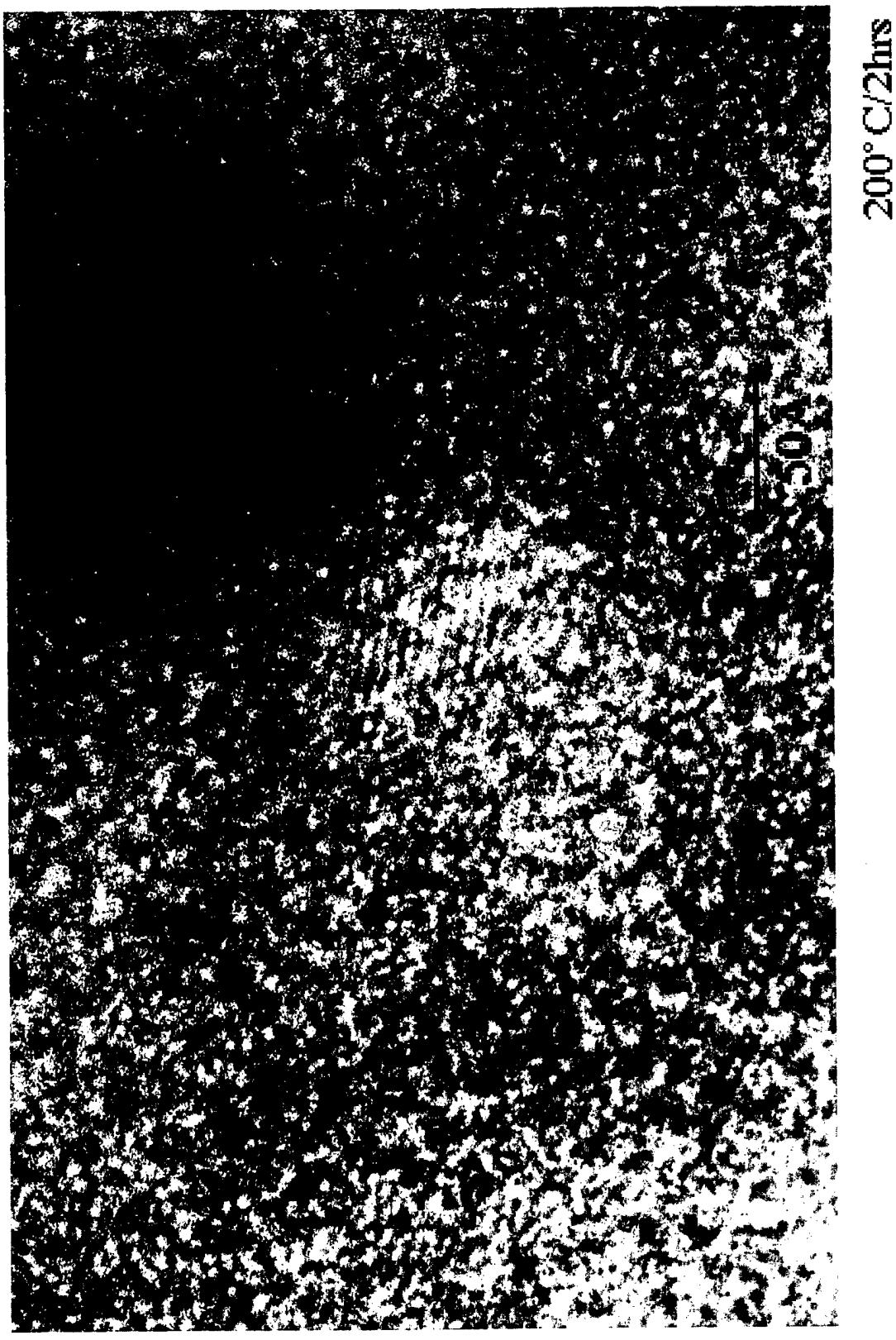

Figure 27 Ferron in 45 TDP-45 $LiNbO_3$-10 SiO_2

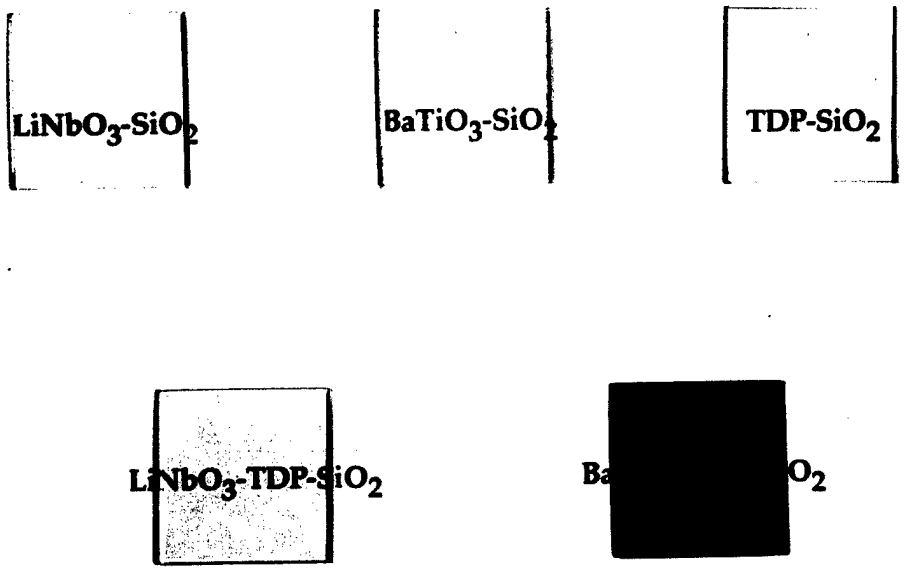

Figure 28 Organic-Inorganic Hybrid Films